Nano-optical and photocurrent characterization of $WSe_2/MoSe_2$ heterostructures

Thomas Darlington[1], Emanuil Yanev[1], Kevin W.C. Kwok[2], Xuehao Wu[3], Natalie Fardian-Melamed[1], Abhay N. Pasupahy[3], James C. Hone[1], P. James Schuck[1]

1. Department of Mechanical Engineering, Columbia University, New York, USA
2. Department of Electrical Engineering, Columbia University, New York, USA
3. Department of Physics, Columbia University, New York, USA
Email: td2583@columbia.edu, pjs2191@columbia.edu

The stacking of two-dimensional (2D) crystals represent a new frontier in materials engineering, offering a degree of control that is not possible with bulk materials. Through choice of 2D material and their twist orientation, fundamental materials parameters can be tuned, such as the bandgap and nonlinear susceptibility. Among the most exciting phenomena currently being studied are effects that arise due to the moiré lattice formed between twisted 2D layers.[1,2] For the Mo- and W- transition metal dichalcogenide (TMD) semiconductors, excitons can become trapped in moiré potential wells, resulting in so-called moiré excitons. However, to date, the existence and properties of moiré excitons have only been inferred spectroscopically due to the sub-wavelength nanoscale nature of moiré lattices in these materials. Real-space nano-optical imaging of moiré excitons has proven difficult due to the inherently low oscillator strength of interlayer excitons and poor alignment of exciton transition dipoles with the antenna mode of common nano-optical probes.[3]

In this presentation, I will show our recent efforts to resolve moiré physics in twisted $MoSe_2/WSe_2$ hetero-bilayers. With combined nano-Raman and nano-photocurrent measurements, we resolve features consistent with domain wall reconstruction known to occur in low-angle twisted TMD heterostructures. Further, we measure sizable photocurrents when pumping at zero bias, which correlates with tip enhanced nano-Raman scattering, suggesting a strong interaction of the interlayer exciton and gap-mode plasmonic mode. Our results demonstrate the feasibility of direct imaging of moiré exciton properties at room temperature at their native length scales and show the potential for new optoelectronic phenomena in TMDs.

References:

[1] Tran, K. *et al.* 2019, *Nature* **567**, 71.
[2] Rosenberger, M. R. *et al.* 2020. *ACS Nano* **14**, 4550-4558.
[3] Sigl, L. *et al.* 2022, *Phys. Rev. B* **105**, 035417.

Ultrabroadband nanocavity of hyperbolic phonon polaritons in 1D-like α-MoO_3

Ingrid D. Barcelos[1], Thalita A. Canassa[2], Rafael A. Mayer[1,3], Flavio H. Feres[1,3], Eynara G. de Oliveira[4], Alem-Mar B. Goncalves[2, 4], Hans A. Bechtel[5], Raul O. Freitas[1], Francisco C. B. Maia[1], Diego C. B. Alves[2,4]

[1] *Brazilian Synchrotron Light Laboratory (LNLS), Brazilian Center for Research in Energy and Materials (CNPEM), Zip Code 13083-970, Campinas, Sao Paulo, Brazil.*
[2] Instituto de Química, *Universidade Federal de Mato Grosso do Sul (UFMS), Zip Code 79070-900, Campo Grande, Mato Grosso do Sul, Brazil.*
[3] *Physics Department, Gleb Wataghin Physics Institute, University of Campinas (Unicamp), 13083-859 Campinas, Sao Paulo, Brazil*
[4] *Instituto de Física, Universidade Federal de Mato Grosso do Sul (UFMS), Zip Code 79070-900, Campo Grande, Mato Grosso do Sul, Brazil.*
[5] *Advanced Light Source, Lawrence Berkeley National Laboratory, Berkeley, California 94720, USA.*
E-mail: Ingrid.barcelos@lnls.br

Polaritons, which are quasiparticles composed of a photon coupled to an electric or magnetic dipole, are a major focus in nanophotonic research of low-dimensional materials. Polaritons can be active in a broad range of the electromagnetic spectrum (meVs to eVs) and exhibit momenta much higher than the corresponding free-space radiation. Hence, the use of high momentum broadband sources or probes is imperative to excite those quasiparticles and measure the frequency-momentum dispersion relations, which provide insights into polariton dynamics. Synchrotron infrared nanospectroscopy[1] (SINS) is a technique that combines the nanoscale spatial resolution of scattering-type scanning near-field optical microscopy with synchrotron infrared radiation, making it highly suitable to probe and characterize a variety of polaritons. Here, the advances enabled by SINS on the study of key different types of polaritons from the THZ to mid-infrared will be described[2,3]. In this work, I will exploit the polaritonic response of α-MoO_3 nanobelts, with reduced dimensionality approaching "1D-like". The polaritons in α-MoO_3 nanobelts feature Fabry-Perot (FP) resonances, primarily from type I HP^2s in the 970-1100 cm^{-1} range. The modes show dependence on the geometric form factor (thickness and width) of the nanobelt and propagate along the [100] crystal direction. In the same crystalline axis, we also show the first infrared nanoimages of type I polaritonic modes in the far-IR band extending from 440 to 490 cm^{-1}. Those analyses are confirmed by a robust convergence among experiment and numerical simulations[3]. Hence, α-MoO_3 nanobelts are presented as an HP^2 nanocavity directly synthesized without the need of lithography or other post-synthetic sculpting processes. This low-dimensional polaritonic material opens new avenues for integrated planar IR photonics, dictating polaritons control and nanoresonators for phonon-enhanced molecular vibrational spectroscopy.

References:

[1] I. D. Barcelos, et al; *Adv. Opt. Mater.* **2020**, *8*, 1.
[2] I. D. Barcelos, et al; *ACS Photonics* **2018**, acsphotonics.7b01017.
[3] F. H. Feres, et al; *Nat. Commun.* **2021**, *12*, 1.

Active Tuning of Highly Anisotropic Phonon Polaritons in Van der Waals Crystal Slabs by Gated Graphene

Gonzalo Álvarez-Pérez[1,2,3], **Arturo González-Morán**[4], **Nathaniel Capote-Robayna**[4], **Kirill V. Voronin**[5], **Jiahua Duan**[1,2], **Valentyn S. Volkov**[5], **Pablo Alonso-González**[1,2], **and Alexey Y. Nikitin**[4,6]

1. Department of Physics, University of Oviedo, Oviedo 33006, Spain.
2. Center of Research on Nanomaterials and Nanotechnology, CINN (CSIC-Universidad de Oviedo), El Entrego 33940, Spain.
3. Department of Physics, Columbia University, New York, NY, 10027, USA
4. Donostia International Physics Center (DIPC), Donostia-San Sebastián 20018, Spain
5. Center for Photonics and 2D Materials, Moscow Institute of Physics and Technology, Dolgoprudny 141700, Russia
6. IKERBASQUE, Basque Foundation for Science, Bilbao 48013, Spain.

E-mail: gonzaloalvarez@uniovi.es

Phonon polaritons (PhPs)─lattice vibrations coupled to electromagnetic fields─in highly anisotropic media [1-4] display a plethora of intriguing optical phenomena, including ray-like propagation, anomalous refraction [5], and optical topological transitions [6], among others, which have potential for unprecedented manipulation of the flow of light at the nanoscale. However, the properties of these PhPs are intrinsically dictated by the anisotropic crystal structure of the host material [6-8]. Although in-plane anisotropic PhPs can be steered, and even canalized, by twisting individual crystal slabs in a van der Waals (vdW) stack [9-12], active control of their propagation via external stimuli, key for their implementation in nano-optical technologies, presents a significant challenge.

Here [13], we report a technology in which anisotropic PhPs supported by biaxial vdW slabs can be tuned actively and in-situ by integrating a gated graphene layer. Excitingly, we predict active tuning of optical topological transitions of the polaritonic IFCs (the optical version of Lifshitz transitions in electronic systems), which enable controlling low-loss canalization of PhPs along different in-plane directions in both single slabs and twisted heterostructures (Fig. 1). Our theoretical and numerical results demonstrate that such tunable topological transitions, leading to canalization of polaritons, are highly dependent on the Fermi level of charge carriers in graphene. Therefore, by simply applying a voltage, the in-plane canalization direction can be controlled in a wide range of angles, opening the door to steer infrared light along specific directions on demand. Excitingly, the propagating properties of the resulting hybrid polaritons, such as propagation length or lifetime, key for applications requiring long-lived light-matter interactions such as strong coupling or mid-infrared (bio)sensing, are not undermined by the ohmic losses in graphene. Apart from their fundamental relevance, our findings pave the way to obtaining optical topological transitions not only actively tunable but also electrically, enabling the integration of anisotropic PhPs with dynamically controllable properties in nano-optoelectronic studies and devices, such as sensors and photodetectors.

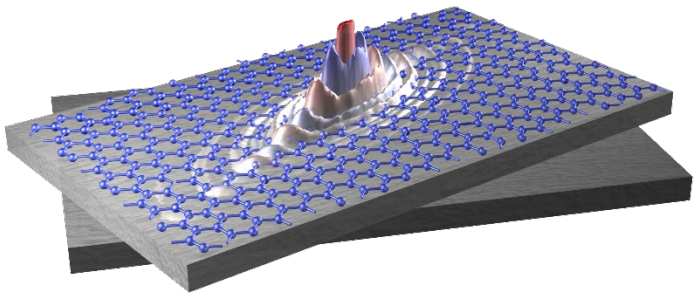

Fig. 1. Phonon polaritons supported by biaxial van der Waals slabs can be tuned actively and in-situ by integrating a gated graphene layer. This enables to guide nanolight along very specific directions by simply applying an external voltage.

References

[1] Dai, S.; et al. 2014. *Science* 343,1125.
[2] Caldwell J. D.; et al. 2014. *Nat. Commun.*, 5, 5221.
[3] Ma, W.; Alonso-González, P.; Li, S.; et al. 2018. *Nature*, 562, 557−562.
[4] Ma, W.; Hu, G.; Hu, D.; Chen, R.; et al. 2021, *Nature* 596, 362–366.
[5] Duan, J.; Álvarez-Pérez, G.; et al. 2021. *Nat. Commun.*, 12, 4325.
[6] Duan, J.; Álvarez-Pérez, G.; et al. 2021. *Sci. Adv.*, 7, eabf2690.
[7] Álvarez-Pérez, G.; Voronin, K. V.; et al. 2019. *Phys. Rev. B*, 100, 235408.
[8] Álvarez-Pérez, G.; et al. 2020. *Adv. Mater.*, 32, 1908176.
[9] Duan, J.; et al. 2020. *Nano Lett.*, 20, 5323–5329.
[10] Hu, G.; et al. 2020, *Nature*, 582, 209−213.
[11] Zheng, Z.; et al. 2020, *Nano Lett.* 20, 5301−5308.
[12] Chen, M.; et al. 2020, *Nat. Mater.* 19, 1307−1311.
[13] Álvarez-Pérez, G.; González-Morán, A.; et al. 2022. *ACS Photonics*. DOI: 10.1021/acsphotonics.1c01549.

Twist-tunable polaritonic nanoresonators

O. G. Matveeva[1†], A. I. F. Tresguerres-Mata[2†], R. V. Kirtaev[1], K. V. Voronin[1], J. Taboada-Gutiérrez[2,3], C. Lanza-García[2], J. Duan[2,3], J. Martín-Sánchez[2,3], V. S. Volkov[1,4], P. Alonso-González[2,3*], A. Y. Nikitin[5,6*]

1. Center for Photonics and 2D Materials, Moscow Institute of Physics and Technology, Dolgoprudny 141700, Russia
2. Department of Physics, University of Oviedo, Oviedo 33006, Spain
3. Center of Research on Nanomaterials and Nanotechnology, CINN (CSIC-Universidad de Oviedo), El Entrego 33940, Spain
4. GrapheneTek, Skolkovo Innovation Center, Moscow 143026, Russia
5. Donostia International Physics Center (DIPC), Donostia/San Sebastián 20018, Spain
6. IKERBASQUE, Basque Foundation for Science, Bilbao 48013, Spain

E-mail: pabloalonso@uniovi.es
† These authors contributed equally to this work

Optical nanoresonators are fundamental building blocks in a number of nanotechnology applications (e.g. in spectroscopy) due to their ability to efficiently confine light at the nanoscale. Recently, nanoresonators based on the excitation of phonon polaritons (PhPs) – light coupled to lattice vibrations – in polar crystals (e.g. SiC, or h-BN) have attracted much attention due to their strong field confinement, high quality factors, and potential to enhance the photonic density of states at mid-infrared (IR) frequencies [1]. Here, we go one step further by introducing PhPs nanoresonators that not only exhibit these extraordinary properties but also incorporate a new degree of freedom: twist tuning, i.e. the possibility to be spectrally controlled by a simple rotation (Fig. 1a). To that end, we both take advantage of the low-loss in-plane hyperbolic propagation of PhPs in the van der Waals crystal α-MoO_3 [2], and realize a dielectric engineering of a pristine α-MoO_3 slab placed on top of a metal ribbon grating, which preserves the high quality of the polaritonic resonances. By simply rotating the α-MoO_3 slab in the plane (from 0 to 45º), we demonstrate by far- and near-field measurements that the narrow polaritonic resonances (with quality factors Q up to 200) can be tuned in a broad range (up to 32 cm^{-1}, i.e. up to ~6 times its full width at half maximum, FWHM ~5 cm^{-1}) (Fig. 1b). Our results open the door to the development of tunable low-loss nanotechnologies at IR frequencies with application in sensing, emission, or photodetection.

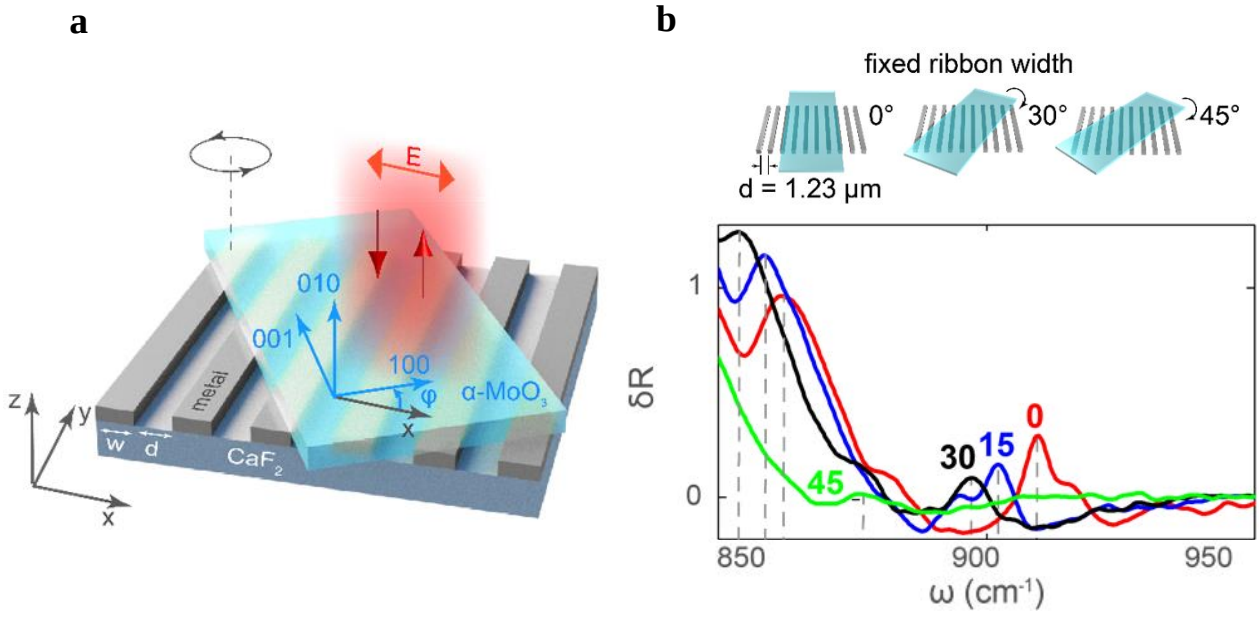

Fig. 1 PhPs nanoresonators in α-MoO_3 defined by placing a pristine α-MoO_3 slab on top of metal ribbons. **a.** Schematics of the studied structure that allows defining the nanoresonators by "dielectric engineering" and controlling them by a twist angle, φ. **b.** Measured relative reflection spectra, δR for twist angles φ =0,15,30 and 45º.

References

[1] Li, Peining. *et al*., 23 Feb 2018, *Science*, Volume 359, 892-896.
[2] Ma, W. *et al*., 25 Oct 2018, *Nature*, Volume 562, 557-562.

Super-resolved identification of nanoscale defects in low-dimensional materials by near-field photoluminescence mapping

Jiatai Huang, Benfeng Bai, Pengyi Feng, Tong Cui, and Hong-Bo Sun
State Key Laboratory of Precision Measurement Technology and Instruments, Department of Precision Instrument, Tsinghua University, Beijing 100084, China
E-mail: hjt20@mails.tsinghua.edu.cn

Low-dimensional materials, especially Monolayer transition-metal dichalcogenides, have emerged as potential candidate materials for next-generation ultra-thin optoelectronics devices. The quality inspection and control in the production of such materials are crucial for their applications, including the detection and identification of the spatial heterogeneity caused by various nanoscale defects.

Here we provide a super-resolved defects identification method based on scanning near-field optical microscopy (SNOM) to explore the photoluminescence (PL) distribution of transferred monolayer WS_2 with sub-diffraction spatial resolution (140 nm) in a large range (10×10 um^2) in ambient environment. By performing topography mapping and photoluminescence nanospectroscopy, the nature of different nanoscale defects in monolayer WS_2, such as the stack, bubble, and wrinkle, can be identified through their light emission properties, which strongly correlate with exciton emission modulation and tensile strain arose from local structural deformations.

According to our study, the PL intensity drops down sharply at the stack region because of the direct-to-indirect bandgap transition when 1L-WS_2 increases to multi-layer[1]. In the bubble region, the peeling off of WS_2 from the substrate and the water molecules trapped inside the bubble induce a relative p-doping effect[2], leading to accumulation of holes in the transferred monolayer WS_2 with electrical neutrality and resulting in the enhancement of the A^T emission and weakening of the A^0 emission. The resonance peak showed relative enhancement and red-shift of about 60% and 5 nm (~15 meV) in the peak of the wrinkle. With the help of high-resolution PL mapping passed above the wrinkle, the red-shift of the PL peak can ascribe to the modified band structure due to the tensile strain induced by the structural deformation[3], and the enhancement of PL intensity at wrinkle peak can be explained by exciton funneling effect[4] since the photo-generated excitons tend to drift to the lower bandgap region.

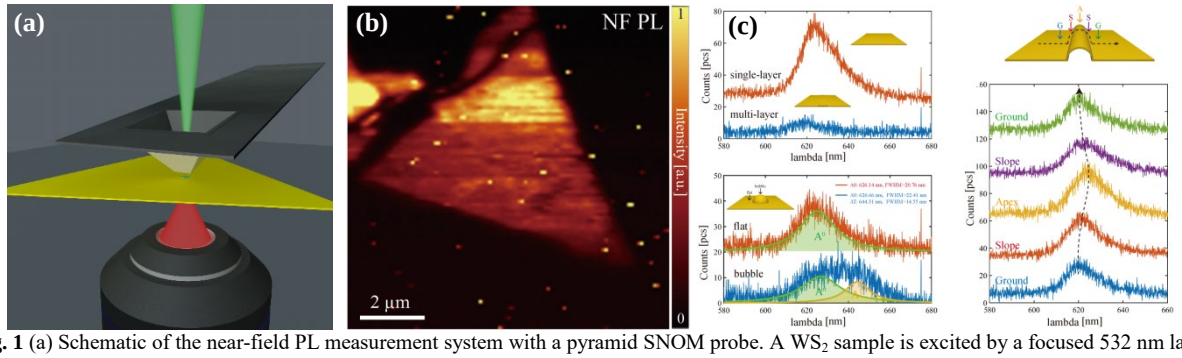

Fig. 1 (a) Schematic of the near-field PL measurement system with a pyramid SNOM probe. A WS_2 sample is excited by a focused 532 nm laser beam through the probe, and the PL signal is collected by a high numerical aperture (NA) objective. The inset shows the optical image of the working probe acquired by a charge-coupled device (CCD), where a focused beam spot is seen. (b) Near-field PL mapping of the sample with integral from 614 nm to 634 nm. (c) near field spectra of various defects in monolayer WS_2.

The presented approach and results deepen the understanding of the spatial emission behaviors in monolayer TMDs and provided a powerful tool for the identification of different local nanoscale defects in low-dimensional materials, which could be necessary for next-generation ultra-thin optoelectronics devices.

References

[1] K. F. Mak, C. Lee, J. Hone, J. Shan, 202 and T. F. Heinz, "Atomically thin mos(2): a new direct-gap semiconductor," Phys Rev Lett 105, 136805 (2010).
[2] Y. Lee, S. J. Yun, Y. Kim, M. S. Kim, G. H. Han, A. K. Sood, and J. Kim, "Near-field spectral mapping of individual exciton complexes of monolayer ws2 correlated with local defects and charge population," Nanoscale 9, 2272–2278 (2017).
[3] D. J. Trainer, Y. Zhang, F. Bobba, X. Xi, S. W. Hla, and M. Iavarone, "The effects of atomic-scale strain relaxation on the electronic properties of monolayer mos2," ACS Nano 13, 8284–8291 (2019).
[4] A. Castellanos-Gomez, R. Roldan, E. Cappelluti, M. Buscema, F. Guinea, H. S. van der Zant, and G. A. Steele, "Local strain engineering in atomically thin mos2," Nano Lett 13, 5361–6 (2013).

Nano-PL mapping of room-temperature strain-localized excitons in array-guided nanowrinkles

Emanuil S. Yanev[1], **Thomas P. Darlington**[1], **Matthew Strasbourg**[2], **Nicholas J. Borys**[2], **James C. Hone**[1], **P. James Schuck**[1]

1. Columbia University, 550 W 120th St, New York, NY 10027
2. Montana State University, 1325 S 6th Ave, Bozeman, MT 59715

emanuil.yanev@columbia.edu

Since their discovery, two-dimensional (2D) materials have garnered much interest in the condensed matter community, both as platforms to investigate new physics, and as promising candidates for a variety of technological advances. Notably, their reduced dimensionality and tunable properties offer intriguing potential for applications in quantum systems and quantum information science. The strain-controlled single-photon emitters (SPEs) observed in 2D semiconductors provide several advantages over SPEs in other materials, which tend to be limited in wavelength tunability, deterministic spatial control, and integrability with other device components.

Motivated by our previous nano-optical studies of strain-localized quantum-dot-like states in tungsten diselenide (WSe_2) [1], this work explores strain-directed and controlled localized emission with the potential of realizing tunable SPEs at room temperature. Here, monolayer sheets of WSe_2 are transferred onto lithographically patterned arrays of sharp conical structures. Owing to the low defect density and single crystal nature of this material, it is able to strongly conform to the substrate features without breaking. In doing so, nanoscale wrinkles are formed around and in-between the cones, with directionality clearly influenced by the array lattice. These highly strained regions can effectively localize excitons, as evidenced by near-field mapping (Figure 1b), and produce similar low-energy emission to that seen in our previous work on nanobubbles [1]. A host of sharp spectral features emerge from these areas at low temperatures, which suggests that the emission is quantum in nature and tunable with strain.

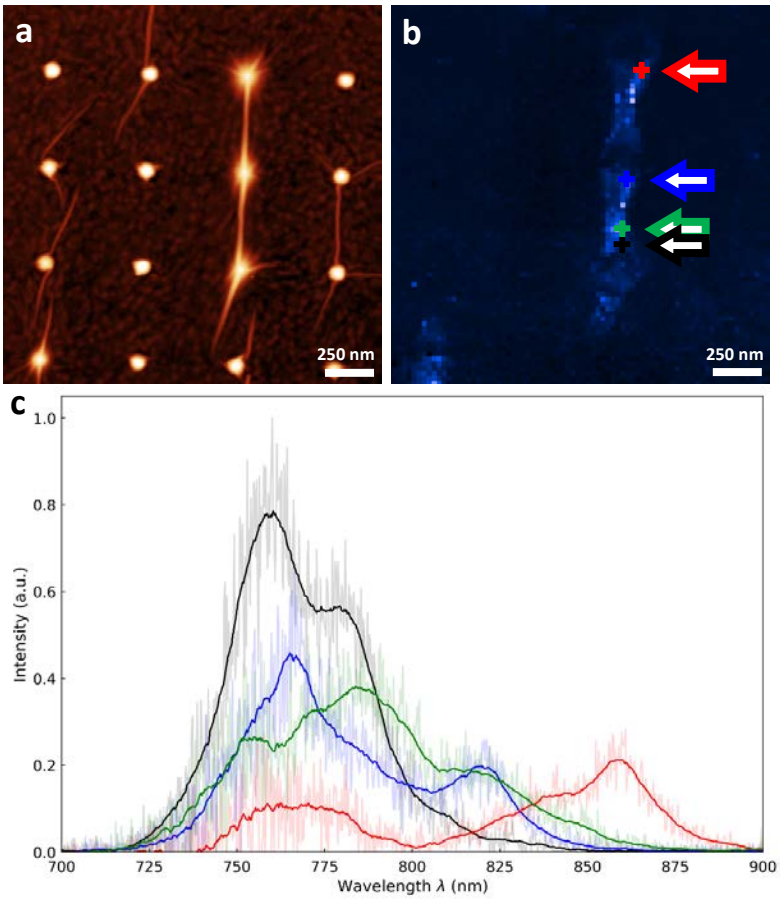

Fig. 1. (a) AFM topography of wrinkles in monolayer WSe_2 on a patterned substrate. (b) Hyperspectral map of the same region showing integrated emission intensity between 780-900 nm. Colored crosses and arrows indicate the locations of the selected spectra shown in (c).

References

[1] Darlington, T.P., Carmesin, C., Florian, M., Yanev, E.S. et al. 2020. *Nat. Nanotechnol*, 15, 854-860.

Tip-enhanced nano-imaging and control of dark excitons in WSe_2

Kathryn Hasz[1], **Zucheng Hu**[1], **Kyoung-Duck Park**[2], **and Markus B. Raschke**[1]

1. Department of Physics, and JILA, University of Colorado, Boulder, CO 80303, USA.
2. Department of Physics, Ulsan National Institute of Science and Technology (UNIST)Ulsan 44919, Republic of Korea
E-mail: kathryn.hasz@colorado.edu

Dark excitons in transition metal dichalcogenides provide new opportunities for optoelectronic devices due to their long lifetimes. SThe strong spin-orbit coupling causes the conduction band to split (**Fig. 1a**), with the dark state not optically active due to a forbidden spin transition, making it difficult to access spectroscopically. It To date, it has primarily been detected using strong magnetic fields at low temperatures to tip the spin to allow for a some degree of optical emission.

Using tip- enhanced photoluminescence (TEPL), we are able to optically detect and control the dark exciton X_D emission as demonstrated in WSe_2. A Here, a gold tip acts as a nanoantenna with polarization parallel to the tip to couple with the out-of-plane moment of the dark exciton (**Fig. 1b**) [1]. In contrast, pPerpendicular polarization is senses only preferentially sensitive to the in-plane moment and thus does not show darkbright moment of the bright excitons X_0. The A tip-sample pico-cavity coupling with the out-of-plane moment allows for Purcell enhancement of $\geq 2x10^3$ ahow much?d Allows for efficient X_D emission of the dark exciton even at room temperature (**Fig. 1c**); and by dynamically controlling the tip-sample distance and associated pico-cavity mode volume we modulate the relative strengths of dark and brightX_0 and X_D emission [2].

RecentPrevious work has demonstrated the ability to detect a dark exciton signal through a pico-cavity with local probe spectroscopy [1]. fFar-field studies have detected evidence of dark excitons, they yet intrinsically provide only a spatial average that would obscures any surface heterogeneities. In order to study and control spatial heterogeneity in dark exciton behavior as also desirable for exciton condensation [3], and associated with nano-bubbles [4] and edges, here we extend this workwe perform correlated to TEPL dark exciton nano-imaging with AFM force spectroscopy with few nanometer spatial resolution.

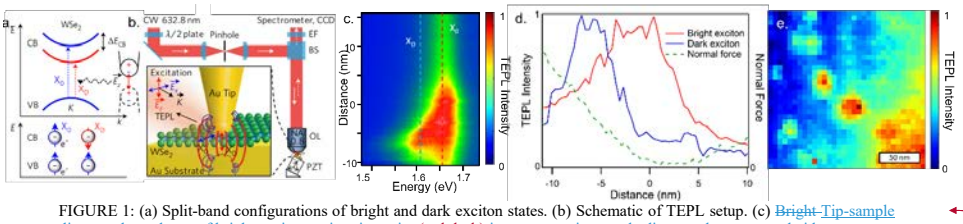

FIGURE 1: (a) Split-band configurations of bright and dark exciton states. (b) Schematic of TEPL setup. (c) Bright Tip-sample distance dependence of bright excitonexciton intensity (red dash) increases as tip-sample distance decreases andwith emergence of pico-cavity enhanced emission of dark exciton satellite peak of the dark exciton (blue dash) in WSe_2 appears. (d) Bright exciton intensity increases before contact, with dark exciton intensity increasing after contactDistinct distance dependence reflecting enhancement and quenching reflecting different X_0 and X_D lifetimes. (c)(e) Pico-cavity Intensity shows spatial variation.X_D TEPL nano-imaging of nano-bubbles of WSe_2 showing spatial heterogeneity of X_D emission with <10 nm spatial resolution.

As seen in Fig. 1c, we see an enhancement of the main Bbright exciton peak (1.65 eV) and a satellite peak corresponding to the dark excitons (1.61 eV) exhibit characteristic tip-sample distance dependent behavior (**Fig. 1c**) with long range field enhancement for X_0, followed by short range pico-cavity induced emission of X_D, transitioning into non-radiative quenching, with relative intensities and characteristic length scales controlled by the competition between Purcell-enhancement, relative lifetimes, temperature activated conversion of X_D to X_0 population, and non-radiative quenchingas the tip approaches the sample surface. The bright exciton peak intensity increases dramatically starting 5-10 nm before the sample surface then begins to quench upon contact, The data are modelled using coupled rate equations [2], and correlated with where contact is defined as the point at which the force on the cantilever transitions from the attractive to repulsive regime (Fig. 1d). In contrast, the dark exciton signal emerges right at the sample surface and increases in intensity for the next 5-10 nm in which force is being applied. It then also begins to quench. We also see aspectral redshifts of both the bright and dark exciton under an applied force, which further allows to relate tip-induced to sample built in local strain suggesting strain as a mechanism to perturbing the excitonic emission in TMD monolayers.

We then image the spatial heterogeneity of the dark exciton intensity revealing . There is a clear variation in strength X_0 and X_D emission of the detected dark exciton intensity (**Fig. 1e**), on few-nanometer length scales, with the strongest X_D intensity occurring around the peakcorrelating in intensity with topographic of nano- of nanoscale bubbles in WSe_2 on Au. Au? What substrate?. The highly strained and non-equilibrium stress state a of WSe_2 nano-bubbles have

Formatted: Space After: 8 pt
Formatted: Bottom: 2.03 cm
Formatted: Line spacing: single
Formatted: Space After: 6 pt, Line spacing: single
Formatted: Space After: 0 pt
Formatted: Font: Bold
Formatted: Indent: First line: 0 cm, Space After: 0 pt
Formatted: Font: Bold
Formatted: Highlight
Formatted: Font: Bold
Formatted: Indent: First line: 0 cm
Formatted: Space Before: 0 pt
Formatted: Indent: First line: 0 cm, Space After: 0 pt
Formatted: Font: Bold
Formatted: Space After: 0 pt
Formatted: Font: Bold
Formatted: Highlight

previously shown a strain-localized exciton developing at nano-bubble edges [5], but the detected intensity of the dark exciton is not confined to the nano-bubble edges.~~t the nano bubbles along with potential polymeric residue could increase light scattering, strengthening the detected intensity of the dark exciton signal. … what do you intend to say?~~

~~I believe there was a paper by Jim Schuck maybe 2-3 years ago who imaged the bright exciton in TEPL and sees emission correlated with the periphery of the bubbles where they strain is largest. I would check into that, in fact include this references, and maybe say that dark exciton emission of bubbles is different from bright excition emission.~~

In summary, in full spatio-spectral nano-imaging of we ~~image and detect~~ dark excitons in WSe_2 w~~.~~ W~~e~~ resolve spatial heterogeneities in ~~both~~ intensity and energy associated with bubbles, ~~and~~ edges, and correlated with local internal and applied strain ~~. By applying strain, we~~ actively ~~change the intensity and energy of the brights~~witching and controlling ~~and~~ dark exciton emission. With better understanding of the sample, structural, and tip-plasmonic coupling ~~conditions for~~ dark excitons ~~, they~~ become ~~more~~ accessible candidates for new optoelectronic applications.

References

[1] K. D. Park, et al. "Radiative control of dark excitons at room temperature by nano-optical antenna-tip Purcell effect," Nat. Nanotechnol, **13**, 59-64 (2018).

[2] M. A. May, et al. "Nanocavity Clock Spectroscopy: Resolving Competing Exciton Dynamics in $WSe_2/MoSe_2$ Heterobilayers," Nano Lett. **21**, 522-528 (2020).

[3] M. Combescot, et al. "Bose-Einstein Condensation in Semiconductors: The Key Role of Dark Excitons," Phys. Rev. Let, **99**, 176403 (2007).

[4] M. Rahaman, et al. "Observation of Room-Temperature Dark Exciton Emission in Nanopatch-Decorated Monolayer WSe_2 on Metal Substrate," Adv. Opt. Mat. **9**, 2101801 (2021)

[5] T. P. Darlinton, et al. "Imaging strain-localized excitons in nanoscale bubbles of monolayer WSe2 at room temperature," **Nat. Nanotechnol. 15, 854 (2020).**

~~[1] Park, K. D.; Jiang, T.; Clark, G.; Xu, X.; and Raschke, M. B. 2018. *Nat. Nanotechnol*, **13**, 59.~~

~~[2] May, M. A.; Jiang, T.; Du, C.; Park, K. D.; Xu, X.; Belyanin, A.; and Raschke, M. B. 2020. *Nano Lett.* **21**, 522.~~

~~[3] Combescot, M.; Betbeder-Matibet,O.; and Combescot, R. 2007. *Phys. Rev. Lett*, **99**, 176403.~~

~~[4] Rahaman, M.; Selyshchev, O.; Pan, Y.; Schwartz, R.; Milekhin, I.; Sharma, A.; Salvan, G.; Gemming, S.; Korn, T.; and Zahn, D.R.T. 2021. *Adv. Opt. Mat.* **9**, 2101801.~~

~~References: add titles, and if not enough space, abbreviate authors as First author, et al.~~

Formatted: Highlight

Formatted: Highlight

Formatted: Indent: First line: 0 cm, Space After: 0 pt

Formatted: Font: Not Bold

Formatted: Space Before: 0 pt

Formatted: Normal

Formatted: Font: 11 pt

Formatted: Font: Not Bold, Highlight

Formatted: Font: Not Bold

Effects of the Dielectric Environment on the Propagation of Phonon Polaritons in Twisted Polaritonic Slabs

Aitana Tarazaga Martín-Luengo[1], Jiahua Duan[1], Christian Lanza[1], Javier Taboada-Gutiérrez[1], Gonzalo Álvarez-González[1], Ana Isabel F Tresguerres-Mata[1], Javier Martín-Sánchez[1], Alexey Y. Nikitin[2], Pablo Alonso-González[1]

1. University of Oviedo, Department of Physics c/ García Lorca, Oviedo, Spain

2. Donostia International Physics Center (DIPC), Donostia-San Sebastián, Spain.

E-mail: aitana555@gmail.com

Phonon polaritons (PhPs) -hybrid light-matter excitations- in van der Waals (vdW) materials present very interesting properties for applications in nanooptics such as high field confinement, low losses and in-plane highly anisotropic propagation [1-3]. Recently, it was shown that by stacking two slabs of α-phase molybdenum trioxide (α-MoO_3) van der Waals material, the propagation of the polaritons along the surface of the top slab can be controlled. Specifically, guiding of PhPs along predetermined directions can be obtained for certain critical twisting angles between the relative crystal directions of the two slabs [4,5]. On the other hand, the propagation of PhPs in a α-MoO_3 slab is strongly affected by the surrounding dielectric environment, as the propagation direction can be switched along previously forbidden directions by inducing a topological transition when the slab is placed on a substrate with a given negative permittivity (the case of silicon carbide) [6].

In this work, we realize combined optical near-field and numerical simulation studies on twisted slabs of α-MoO_3 on a silicon carbide substrate. Particularly, we study the dependence of the relative crystal axes orientation between the two slabs on the propagation of the PhPs, and as a function of the illumination frequency. We find a topologically induced transition in the propagation of PhPs along the surface of the bilayer from a nearly isotropic regime to a highly anisotropic ray-like propagation. Our results provide in-depth fundamental knowledge about the propagation of PhPs in twisted slabs placed on different dielectric environments.

References

[1] Dai,S., Fei, Z., Ma, Q., Rodin, A.S., Wagner, M., McLeod, A.S., Liu, M.K., Gannett, W., Regan, W., Watanabe, K, Taniguchi, T., Thiemens, M., Dominguez, G., Castro Neto, A.H., Zettl, A., Keilmann, F., Jarillo-Herrero, P., Fogler, M.M., Basov, D.N. 2014. *Science*, 343, 1125.

[2] Ma, W., Alonso-González, P., Li, S., Nikitin, A.Y., Yuan, J., Martín-Sánchez, J., Taboada-Gutiérrez, J., Amenabar, I., Li, P., Vélez, S., Tollan, C., Dai, Z., Zhang, Y., Sriram, S., Kalantar-Zadeh, K., Lee, S.T., Hillenbrand, R., Bao, Q. 2018. *Nature*, 562, 557.

[3] Zheng, Z., Xu, N., Oscurato, S.L., Tamagnone, M., Sun, F., Jiang, Y., Ke, Y., Chen, J., Huang, W., Wilson, W.L., Ambrosio, A., Deng1, S., Che, H. 2019. *Sci. Adv.*, 5, eaav8690.

[4] Duan, J., Capote-Robayna, N., Taboada-Gutiérrez, J., Álvarez-Pérez, G., Prieto, I., Martín-Sánchez, J., Nikitin, A.Y., Alonso-González, P. 2020. *Nano Lett.*, 20, 5323.

[5] Hu, G., Ou, Q., Si, G., Wu, Y., Wu, J., Dai, Z., Krasnok, A., Mazor, Y., Zhang, Q., Bao, Q., Qiu, C.W., Alù, A. 2020. *Nature*, 582, 209.

[6] Duan, J., Álvarez-Pérez, G., Voronin, K.V., Prieto, I., Taboada-Gutiérrez, J., Volkov, V.S., Martín-Sánchez, J., Nikitin, A.Y., Alonso-González, P. 2021. *Sci. Adv.*, 7, eabf2690.

Brobdingnagian photon bunching in cathodoluminescence of excitons in WS_2 monolayer

Saskia Fiedler[1], Sergii Morozov[1,2], Leonid Iliushyn[2,3], Sergejs Boroviks[1], Martin Thomaschewski[1], Jianfang Wang[4], Timothy J. Booth[2,3], Nicolas Stenger[2,5], Christian Wolff[1], and N. Asger Mortensen[1,2,6]

1. Center for Nano Optics, University of Southern Denmark, Campusvej 55, Odense 5230, Denmark
2. Center for Nanostructured Graphene, Technical University of Denmark, DK-2800 Kongens Lyngby, Denmark
3. Department of Physics, Technical University of Denmark, DK-2800 Kongens Lyngby, Denmark
4. Department of Physics, The Chinese University of Hong Kong, Shatin, Hong Kong SAR, China
5. Department of Photonics Engineering, Technical University of Denmark, DK-2800 Kongens Lyngby, Denmark
6. Danish Institute for Advanced Study, University of Southern Denmark, Campusvej 55, DK-5230 Odense M, Denmark

E-mail: semo@mci.sdu.dk

Cathodoluminescence spectroscopy in conjunction with second-order auto-correlation measurements of $g_2(\tau)$ allows to extensively study the synchronization of quantum light sources in low-dimensional structures [1]. Co-existing excitons in two-dimensional transition metal dichalcogenide monolayers provide a great source of identical quantum emitters which can be simultaneously excited by an electron. In this article, we demonstrate large photon bunching with $g_2(\tau)$ up to 156±16 of a tungsten disulfide monolayer, exhibiting a strong dependence on the electron-beam current density. To further improve the excitation synchronization and the electron-emitter interaction, we show exemplary that the careful selection of a simple and compact geometry - a thin, monocrystalline gold nanodisk - can be used to realize a record-high bunching $g_2(0)$ of up to 2152±236 [2]. This approach to control the electron excitation of excitons in a WS_2 monolayer allows for the synchronization of quantum emitters in an ensemble, which is important to further advance quantum information processing and computing technologies.

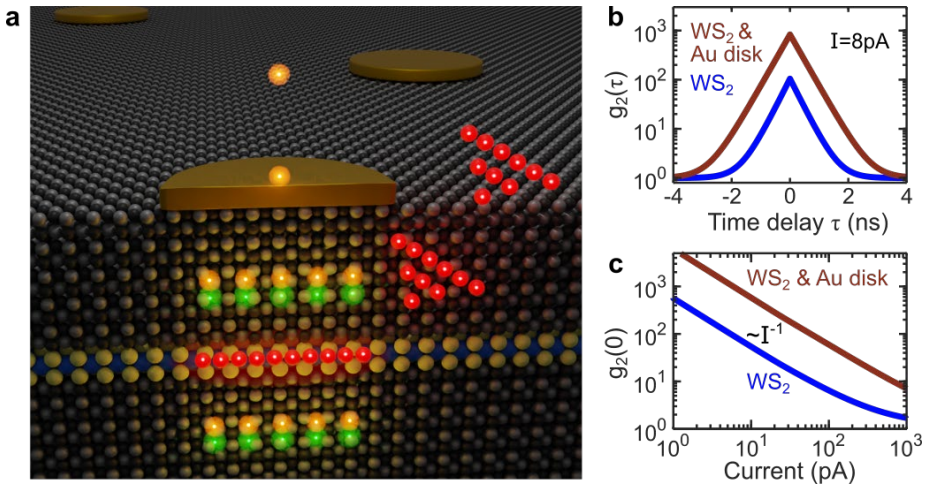

Fig. 1 a Artistic view for generation of highly bunched light. A high-energy electron generates multiple electron-hole pairs in hBN sandwich, which experience synchronized radiative recombination in the WS_2 monolayer. **b** Strong photon bunching in hBN-encapsulated WS_2 monolayer and the same structure with a gold nanodisk measured at the same electron beam current (8 pA) and acceleration voltage (30 kV). **c** The photon bunching amplitude $g_2(0)$ is limited by the lowest electron beam current attainable by the instrument, while the addition of a gold nanodisk can further boost $g_2(0)$ through the local manipulation of electron beam current.

.

References

[1] Meuret S., Adv. *Imaging Electron Phys.* 215, 47 (2020).
[2] Saskia Fiedler, Sergii Morozov. Leonid Iliushyn. Sergejs Boroviks, Martin Thomaschewski, Jianfang Wang, Timothy J. Booth, Nicolas Stenger, Christian Wolff, and N. Asger Mortensen, *arXiv:2111.07596*, (2021).

In-situ optical tracking of memristive switching in 2D materials

Joanna Symonowicz[1,2], **Giuliana Di Martino**[1]

1. Department of Materials Science and Metallurgy, University of Cambridge, Cambridge, UK
2. Cavendish Laboratory, University of Cambridge, Cambridge, UK
E-mail: jks68@cam.ac.uk

Up to 80% of the computing energy is consumed in the data-transfer between logic and memory units [1]. Resistive switching memories enable modern in-memory computing architectures, where memory and logic are no longer separated, avoiding inefficient shuttling of information. Materials suitable for memristive switches are thus in high demand and among the contenders are MoS2 and h-BN nanosheets. However, their switching mechanisms are still debated [2,3].

In our work, we tightly confine light, i.e. plasmonic hotspots, within the electrically switched nanosheets [4]. This allows to optically track in-situ and in real-time morphological changes happening in nanoscale Au/MoS2/Au and Au/h-BN/Au memristive cells. This novel non-destructive and fully optical technique enables Raman, darkfield scattering, and photoluminescence analysis from single-digit nanometer areas, hence providing unprecedented insights into the underlaying mechanism of the MoS2 and h-BN memristive switching.

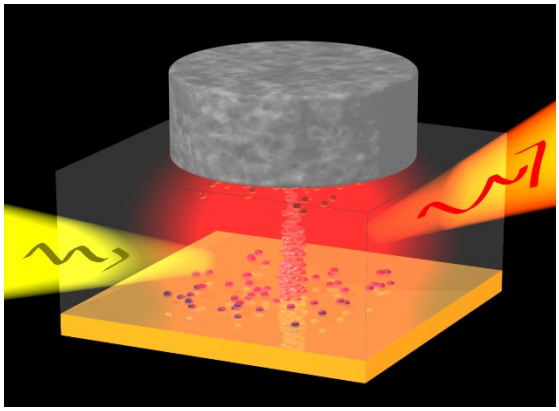

Fig. 1 A schematics of our technique used to optically track morphological changes occurring in nanosheets upon voltage changes.

References

[1] Miller, D. A. B. (2009) *IEEE Proceedings* 97, 7, 1166.
[2] Hus, S. et al., (2021) *Nature Nanotechnology* 16, 58–62.
[3] Ge, R. et al., (2020) *Advanced Materials* 33, 7, 2007792.
[4] Di Martino, G. et al., (2020) *Nature Electronics* 3, 687.

Orientation-Dependent Interaction between the Magnetic Plasmons in Gold Nanocups and the Excitons in WS_2 Monolayer and Multilayer

Ruoqi Ai, Xinyue Xia, Jianfang Wang*

Department of Physics, The Chinese University of Hong Kong, Shatin, Hong Kong SAR, China

E-mail: jfwang@phy.cuhk.edu.hk

Typically, a quantum emitter in free space cannot interact strongly with photons due to the large mismatch between the emitter size and the light wavelength. Metallic nanostructures, which can support localized surface plasmon resonances and concentrate light into the sub-wavelength scale, are highly potential candidates for enhancing the light–matter interactions [1]. The interaction between plasmons in metal nanostructures and excitons in two-dimensional transition-metal dichalcogenides has attracted tremendous attention due to its fundamental importance in cavity quantum-electrodynamics research and great potential in quantum information applications [2]. In this work, we investigate the interaction between the magnetic plasmons in differently orientated Au nanocups and excitons in WS_2 monolayer and multilayer (Fig. 1a). By varying the orientation and size of the Au nanocups, spectral overlap between the magnetic plasmon mode of the Au nanocups and the excitons of WS_2 monolayer is achieved (Fig. 1b and 1c, upper and middle panel). Different resonance coupling regimes have been reached with the individual nanocups by adjusting the nanocup orientation on WS_2 monolayer, resulting in weak to strong coupling (Fig. 1c, lower panel). The finite-difference time-domain (FDTD) shows that the strong coupling for the downward configuration has benefited from the magnetic mode, which can induce the strong near-field electric enhancement in the WS_2 layer and intensely interact with the in-plane excitons. By varying the diameter and opening size of the downward Au nanocup, the magnetic plasmon resonance can be successfully adjusted to accurately match the excitons of WS_2 monolayer, giving rise to a splitting energy up to 106 meV for the magnetic plasmon–exciton system. Both the simulated scattering and absorption spectra indicate that the system is in the strongly coupled regime. The coupling strength also increases as the number of layers increases due to more excitons participating in the coupling. The magnitude of the coupling strength increases with the number of layers and then saturates at ~4 layers. Our study provides a feasible approach toward the realization of different coupling regimes in such an individual particle/exciton transition system.

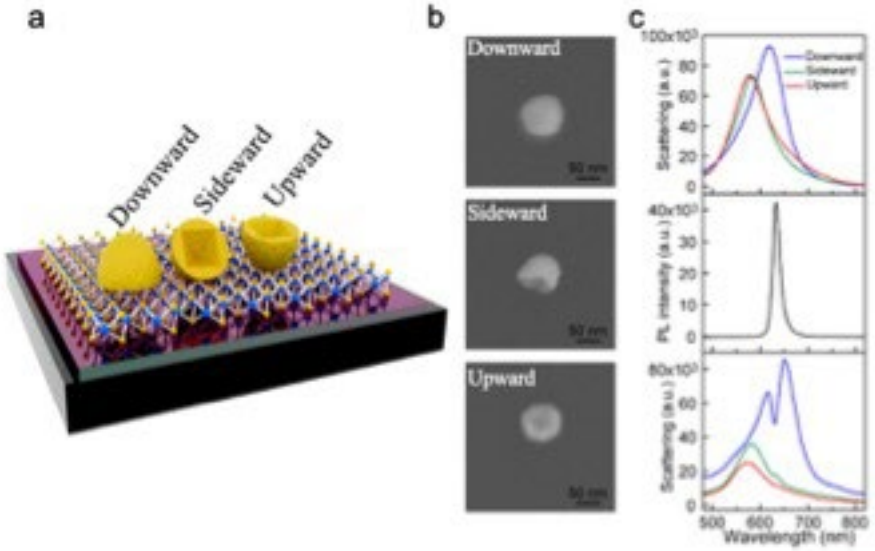

Fig. 1 Fig. (a) Schematic illustrating the heterostructures composed of Au nanocups in different orientations on the WS_2 monolayer. (b) SEM images of the three representative Au nanocups in the three typical orientations on WS_2 monolayer. (c) Measured scattering spectra of the three differently orientated Au nanocups on the SiO_2 substrate (upper), PL spectrum of WS_2 monolayer (middle), and scattering spectra of the three differently orientated Au nanocups coupled to WS_2 monolayer (lower), whose SEM images are shown in (b).

References

[1] Hugall, J. T.; Singh, A.; Hulst, N. F. 2018. *ACS Photonics*. 5, 43.

[2] Torma, P.; Barnes, W. L. 2015. *Rep. Prog. Phys*. 78, 013901.

Manipulating the fluorescence contrast in liquid-gel phases

Jia-Ru Yu[1, 2], He-Chun Chou[1], Wei-Ssu Liao[2], and Chi Chen1[2]

1. Research Center for Applied Sciences, Academia Sinica, Taipei, 115, Taiwan
2. Department of Chemistry, National Taiwan University, Taipei, 106, Taiwan
*e-mail: chenchi@gate.sinica.edu.tw

Fluorescence tagging of the supported lipid bilayers (SLBs) is an essential technique for imaging the particular components in the biological membrane. It is generally believed that the tagged lipids would participate in the liquid-disordered (fluid) phase rather than the liquid-ordered (gel) phase. Such partition behavior of tagged lipids usually guides the interpretation of the fluorescence-bright or dark domain on the membrane. Here, we employ our homebuilt liquid-phase scanning near field microscopy (SNOM) to study lipid bilayers [1] (Fig. 1 (a) and (b)). A heating circuit and temperature feedback is equipped in the liquid cell for observing the movement and phase segregation of lipids under temperature control. We can manipulate local lipid molecules from gel phase to fluid phase by the *a*-SNOM tip, which caused the reverse of fluorescence contrast (Fig. 1 (c)). It demonstrates that there is no preferable partition for the fluorescence tag in the fluid or gel phases. The packing and relative motion among neighbor lipids determine the dipole orientation and lead to distinct EET efficiency between the gel and fluid phase. Our results not only reveal the fundamental issue of fluorescence tag partition but also offer a practical guide in interpreting the fluorescence contrast.

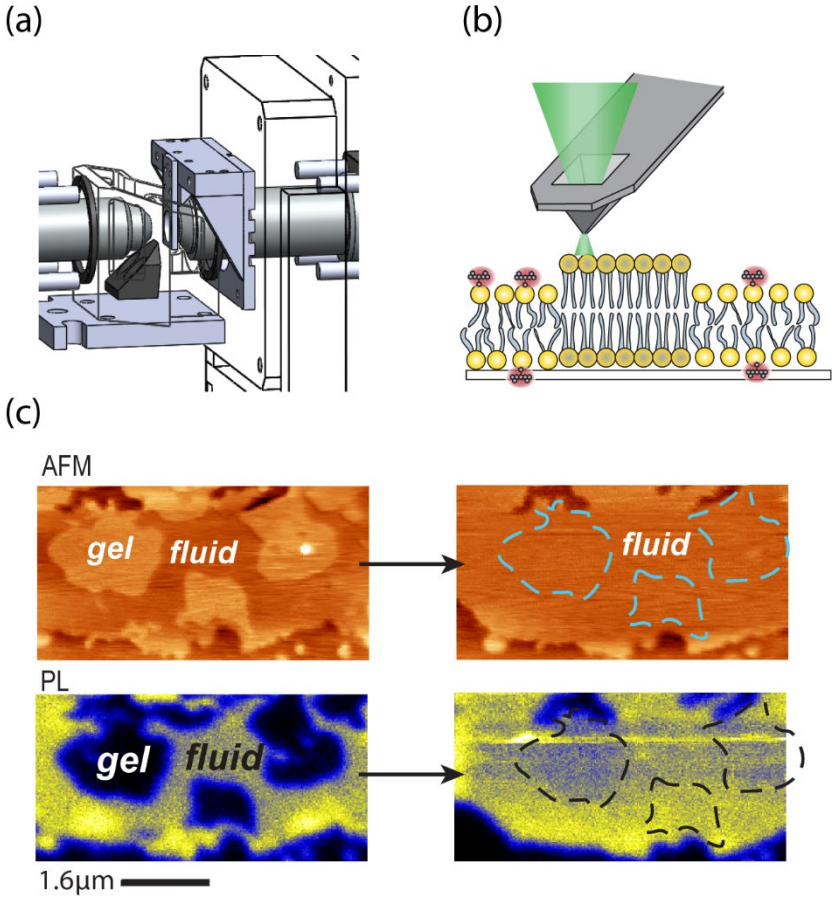

Fig. 1 (a) Schematic illustration of the homebuilt liquid-phase SNOM system. (b) Schematic illustration of a *a*-SNOM tip to scan lipid bilayers. (c) The sequential *a*-SNOM images of the DPPC:DOPC = 1:1 SLB with 3% Texas red-DHPE fluorescence probe. Top row is the *a*-SNOM topography and the bottom row is the simultaneous recorded *a*-SNOM fluorescence intensity map.

References

[1] Yu, J.R.; Chou, H.C.; Yang, C. W.; Liao, W. S.; Hwang, I. S.; Chen, C 2020, *Rev. Sci. Instrum.* 910, 73703.

Imparting spectrally selective optical properties to metallic substrates through surface engineering

Sraboni Dey and J. Mitra

School of Physics, Indian Institute of Science Education and Research, Thiruvananthapuram-695551, India

E-mail: srabonidey20@iisertvm.ac.in

Recent advancements in nanoscience and nanotechnology have revolutionized applications of plasmonics and photonics. Direct optical excitation of surface plasmons on nanostructures and thin films with free carriers brings about unique ways to influence light matter interactions. Novel optical materials, innovative new devices have been developed with significant potential to contribute to the growing technology [1] where degenerately doped, wide band gap metal oxides such as Al doped ZnO, ITO, doped CdO etc can replace metals as plasmonic materials. This is enabled by their controllable carrier density that allows tuning of their dielectric to metallic transition wavelength known as epsilon near zero (ENZ) wavelength (λ_{ENZ}) [2]. A niche application of ENZ materials and their plasmonic properties is evidenced in the development of spectrally selective coatings, where the optical property of a reflecting metallic surface is XXX with the ability to selectively absorb light below a tailored wavelength and reflect at higher wavelengths. Such coatings have potential applications in areas such as solar energy conversion, thermal management, radiative cooling, smart windows etc [3]. The challenges being the overall complexity and thickness of the coatings along with their angular dependence of their spectral selectivity.

Here we demonstrate using how surface engineering can impart spectrally selective optical properties to a ubiquitous substrate like stainless steel (SS) from visible to near IR. The surface engineering has been executed by coating a tri-layer thin film (ITO/Cr/Cr_2O_3) each of optimal thicknesses on SS with an elementary periodic grating of ITO nanostructures of optimized dimensions over the substrate. Investigated from 400 – 4000 nm the coated substrate shows high average absorption (~90%) over the entire visible up to a particular wavelength λ_0 beyond which the reflectivity becomes ~ 80%. In other words, the reflection coefficient is like a "step function" at that particular wavelength λ_0 (here around ~1670 nm), which is an omnidirectional feature realized between 0° to 60°, as shown in Fig 1b. Importantly, λ_0 can be tuned using proper selection of materials which has been showcased here through the utilization of an ENZ material i.e. ITO both in thin film and nanostructured form supported by the absorbing coating underneath.

The focus is not only on the optical response which has been achieved but also on the roles played by the individual building blocks of this system which has been depicted in Fig 1c. The power dissipation calculation performed for various wavelengths from visible to IR exhibits the contribution of the underlying Cr/Cr_2O_3 coatings on stainless steel and proves its significance in bringing down the reflectivity to nearly 10% in the visible regime and also for ITO in playing the major role as the reflector in the near IR. Overall, the opportunistic employment of these materials in the right forms and dimensions has proven to develop this unique response. Therefore, the system that has been developed not only demands direct applications in optical devices but also exploring it from the fundamental material research point of view.

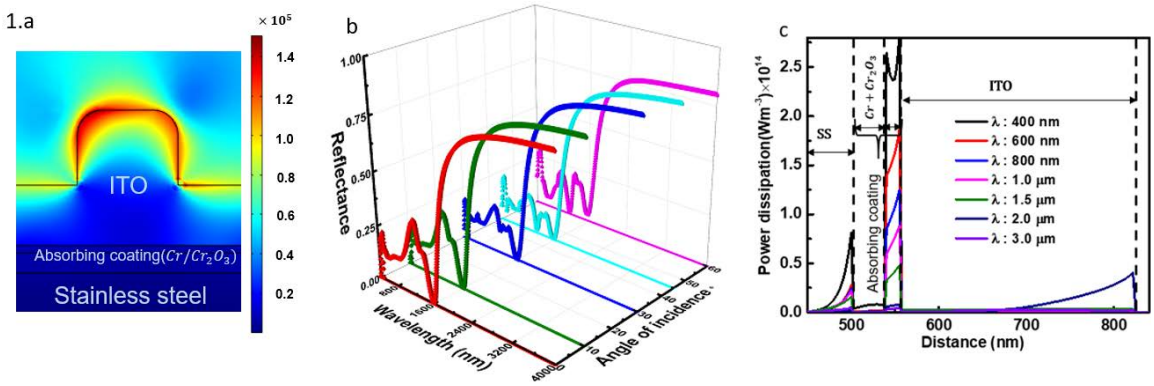

Fig. 1a. Magnitude of electric field variation across the system, b. Simulated reflectance spectra, c. Power dissipation across different layers

References

[1] Halas, Naomi J., *2010*, *Nano Letters*, 10, 3816-3822.

[2] Johns, Ben Puthoor, Navas Meleth Gopalakrishnan, Harikrishnan Mishra, Akhileshwar Pant, Ravi Mitra, J., *Journal of Applied Physics,2020,* 127,043102.

[3] Li, Yang Lin, Chongjia Huang, Jingyuan Chi, Cheng Huang, Baoling,, *Global Challenges, 2021*,5,2000058.

Light-controlled microdroplet robot on nanophotonic substrate

Masayuki Naya[1,2], **Nanami Ohhara**[1], **Akinobu Yamaguchi**[2] **and Toshiharu Saiki**[1]

1. Graduate school of Science and Technology, Keio University, 3-14-1, Hiyoshi, Kohoku-ku,Yokohama, Kanagawa 223-8533, Japan
2. Laboratory of Advanced Science and Technology for Industry, University of Hyogo, 3-1-2 Kouto, kamigori, Ako-gun, Hyogo 678-1205, Japan
E-mail: masa@naya-lab.com

The formation of microdroplets and their behavior are important subjects for the investigation of the origin of life [1] and applications such as precise material transport. Recently, the artificial formation of a micro-droplet driven by Marangoni convection, which is generated by irradiating a laser beam onto a thin film of light-absorbing liquid, has been reported [2,3]. We have found that artificial droplet generation is possible even with non-light-absorbing liquid by using light-absorbing substrates such as a GeSbTe film, a gold film, and plasmonic-films. Furthermore, we found that the generated droplet performs self-excited motion such as vibration and rotation.

Figure1 shows the experimental setup. By sandwiching a volatile liquid (ethanol) mixed with a small amount of non-volatile polymer liquid (PEG) between a gold substrate and a glass substrate, a reservoir of liquid and an air gap with wetting film are created between the substrates. A sessile droplet can be formed on a gold film surface in the air gap area by irradiating a 532 nm CW laser spot (Fig. 2 and Fig. 3). We found that the droplet moves spontaneously even when the laser spot is fixed. The mechanism of this phenomenon is thermal Marangoni convection due to the local heating by the optical absorption of the gold film and the solutO Marangoni convection due to the local increase of PEG concentration caused by evaporation of ethanol in the light-irradiated area.

Since the concentration of PEG in the droplet generated by the soluto Marangoni convection should be higher than that in the wetting film surrounding the droplet, the droplet formation involves liquid-liquid phase separation. The liquid-liquid phase separation is a phenomenon, in which a polymer in a liquid moves such as due to thermal interactions, causing the separation into a polymer-rich phase and a dilute phase [4]. It has attracted strong attention due to its relevance to the origin and activities of life and its potential applications including drug delivery in cells. Although inducing phase separation by chemical reaction is common, it is not applicable to generating and controlling single droplets, making it difficult to precisely analyze the phenomenon. In contrast to this, our method enables creation, annihilation, and transportation of single droplets at a desired position. More interestingly, we found that the droplets exhibit spontaneous motion such as vibration and rotation. These phenomena suggest the possibility of realizing a droplet robot controlled by light. A possible application includes collection and transport of targeted nanoparticles. We will also demonstrate that microdroplets can be generated by irradiating white light over a wide area on a patterned nanophotonic substrate.

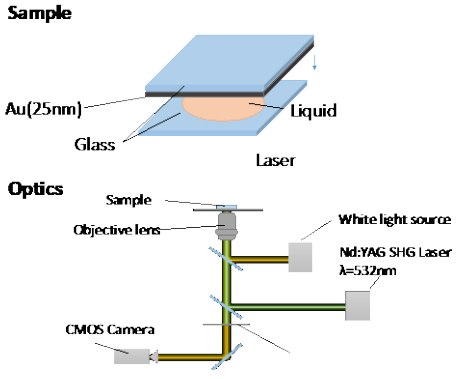

Fig.1 Experimental setup for droplet formation

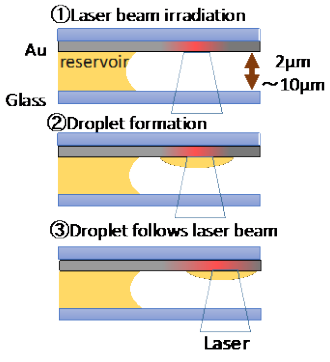

Fig.2 Droplet formation process

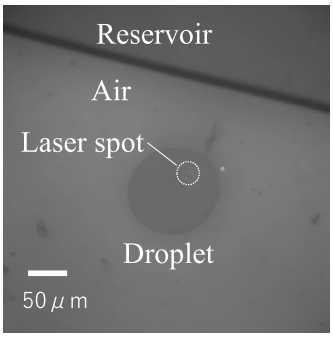

Fig.3 Optical Microscope image of droplet

References

[1] D. Twicker, R. Seyboldt, C.A. Weber, A.A. Hyman and F. Julicher, 2017, Nature Physics, 13, 408–413.
[2] N.A. Ivanova and B.A. Bezuglyi, 2007, Colloid J., 69, 735–740 .
[3] K.A. Tatosova, A.Y. Mallyuk and B.A. Bezugly, 2017, Colloid and Surface A., 521, 22–29.
[4] C.D. Keating, 2012, ACC Chem. Res. 45, 2114–2124.

“Photonics in Canada”

By: Nikki Bulgarea and Robert Corriveau, Photons Canada.

As the main organization representing the Canadian photonics industry and researchers, Photons Canada is organizing Events like, workshops, webinars, and networking events with the objective of increasing, fostering and accelerating the collaboration between industry, R&D centres and university researchers ensuring Canada growth through innovation in photonics.

In 2021, Photons Canada has initiated and developed a report looking at strength, weakness, opportunity, and threat (SWOT) analysis for the following six technologies in Canada:

- biophotonics,
- Imaging, sensors and fusion,
- Laser processing for advanced manufacturing,
- Photonics integrated circuits,
- photovoltaics and
- quantum technologies.

It was concluded that these photonics technologies are present and covered in Canada.

In 2022, we will proceed with a more detailed SWOT analysis by region: Western Provinces, Ontario, Quebec and the Maritimes.

After an overview of the global photonics in Canada, the different aspects for the Western Provinces SWOT analysis will be presented for an open discussion with the participants.

Ultrasensitive analysis of nano-matter via scattering: from single proteins and viruses to sub-cellular features

Vahid Sandoghdar
Max Planck Institute for the Science of Light,
Max-Planck-Zentrum für Physik und Medizin,
91058 Erlangen, Germany
Email: vahid.sandoghdar@mpl.mpg.de

The last two decades have witnessed the insatiable potential of optical techniques for sensitive studies. Optical detection of small nanoparticles and single molecules have often relied on fluorescence, but limited photophysics and the need for labeling pose severe restrictions for the broad application of this approach. The ubiquitous process of Rayleigh scattering offers a powerful alternative. Although the common intuition might be that detection of individual nanoparticles and single molecules is not within reach via the measurement of their Rayleigh scattering, interferometric scattering (iSCAT) microscopy introduced in 2004 has demonstrated the contrary [1]. Indeed, it is now possible to reach a remarkable real-time detection sensitivity down to single unlabeled proteins [2]. In this presentation, I will present the most recent advances in iSCAT analysis, reaching an exquisite sensitivity for detecting single unlabeled bio-particles as light as 10 kDa [3,4]. I also discuss new results in three-dimensional imaging and tracking of sub-cellular structures in live cells [5].

References:

1- R. W. Taylor and V. Sandoghdar,
Interferometric Scattering Microscopy: Seeing Single Nanoparticles and Molecules via Rayleigh Scattering,
Nano Letters **19,** 4827-4835 (2019).

2- M. Piliarik and V. Sandoghdar, Direct optical sensing of single unlabelled proteins and super-resolution imaging of their binding sites, *Nature Communications* **5** 4495 (2014).

3- A. D. Kashkanova, M. Blessing, A. Gemeinhardt, D. Soulat, V. Sandoghdar,
Precision size and refractive index analysis of weakly scattering nanoparticles in polydispersions,
Nature Methods **19,** 586-593 (2022)

4- M. Dahmardeh, H. Mirzaalian Dastjerdi, H. Mazal, H. Köstler, V. Sandoghdar,
Self-supervised machine learning pushes the sensitivity limit in label-free detection of single proteins below 10 kDa,
https://doi.org/10.21203/rs.3.rs-1635524/v1 (2022).

5- M. Küppers, D. Albrecht, A. D. Kashkanova, J. Lühr, V. Sandoghdar,
Confocal Interferometric Scattering Microscopy Reveals 3D Nanoscopic Structure and Dynamics in Live Cells,
https://doi.org/10.21203/rs.3.rs-1690188/v1 (2022).

High throughput imaging of thermal conductivity and interfacial thermal conductance with nanoscale resolution

Andrea Centrone[1], **Mingkang Wang,**[1,2] **Georg Ramer,**[1,2] **Vladimir Aksyuk**[2]

1. National Institute of Standards and Technology, Gaithersburg, MD 20899 USA
2. University of Maryland, College Park, MD 20742, USA
E-mail: andrea.centrone@nist.gov

Accurate knowledge of thermal conductivity (η) and interfacial thermal conductance (G) at the nanoscale is critical for engineering thermoelectrics, memristors and other advanced electronic devices and for studying thermal transport in nanostructured or quantum materials. State of the art, time-domain thermoreflectance (TDTR) is a high signal-to-noise, pump-probe, technique that measures η and G by reconstructing the sample time-domain photothermal expansion as a function of the probe delay time. However, TDTR spatial resolution is limited to the micrometer scale and requires long measurement times (≈ 120 s per point), even when coating the sample with a metallic (reflective) transducer layer to increase its sensitivity. Photothermal induces resonance (PTIR) [1,2] is a scanning probe technique that uses the tip on an AFM to transduce the sample photothermal expansion and to enable IR spectroscopy at the nanoscale. However, conventional AFM probes do not have sufficient sensitivity or bandwidth to capture the fast sample thermalization that could be used to extract the sample thermal properties at the nanoscale.

Here, we develop an optomechanical cantilever probe and customize PTIR setup to directly capture at once the entire time-domain sample thermal expansion dynamic due to the absorption of IR laser pulses with nanoscale resolution. This novel setup can measure thermal dynamic events with ≈ 10 ns temporal resolution, ≈ 35 nm spatial resolution, and high sensitivity concurrently, thanks to a very low detection noise (≈ 1 fm/Hz1/2) over a wide (> 100 MHz) bandwidth. Such high sensitivity, wide bandwidth measurement enables fast data acquisition (≈ 20 ms) and nanoimaging of η and G with a throughput ≈ 6000 × faster than macroscale-resolution TDTR and ≈ 500000 × faster than for measurements with conventional AFM cantilevers. This feat is achieved by improving the nanophotonic AFM transducers design (≈ 5 × higher lateral stiffness, ≈ 3 × lower measurement noise, and ≈ 4 × larger bandwidths than previous attempts [3]), by integrating a novel wavelength-tunable IR excitation laser with a 200 × faster repetition rate (200 kHz) and by developing a custom FPGA data acquisition system that digitizes and process the data at the high rates (0.8 GHz) required by fast scanning.

As a proof-of-principle demonstration, we obtain 100 × 100 pixel maps of η and G in 200 s with a small relative uncertainty (Δη ≈ 10 % and ΔG ≈ 5 %) on a ≈ 3 μm wide polymer particle. Importantly, such measurements do not require extensive probe calibration (as for other AFM-based measurements) or a metallic transducer layer on the sample (as for TDTR).

This work paves the way to study fast thermal dynamics in materials and devices with nanoscale resolution, which is critical, for example, to study the thermal properties of grain boundaries and of filaments in memristive devices.

References

[1] Centrone, A., *Annu. Rev. Anal. Chem.* **2015,** *8* (1), 101-126.
[2] Kurouski, D. ; Dazzi, A.; Zenobi, R. ; Centrone, A, *Chem. Soc. Rev.*, **2020**, 49, 3315-3347
[3] Cahe, J.; et al, *Nano Lett.* **2017**, 17, 5587–5594

Bloch Surface Waves for surface enhanced Mid-Infrared spectroscopy

Raffaella Polito[1], Agostino Occhicone[1], Marialilia Pea[2], Alberto Sinibaldi[1], Francesco Mattioli[2], Sara Cibella[2], Andrea Notargiacomo[2], Alessandro Nucara[1], Paolo Biagioni[3], Francesco Michelotti[1], Michele Ortolani[1], and Leonetta Baldassarre[1]

[1]Sapienza University of Rome, Rome, 00185 Italy
[2]CNR – Institute for Photonics and Nanotechnologies, Rome, 00154 Italy
[3]Politecnico di Milano, Milano, 20133 Italy
E-mail: raffaella.polito@uniroma1.it

Mid-Infrared (mid-IR) spectroscopy in the 2-20 μm spectral region could play a relevant role in the field of label-free biosensors, being a valuable tool for the chemical identification of molecular species and even for probing the molecule conformations in some cases, due to the specificity of mid-IR vibrational fingerprints. Nevertheless, the long wavelengths of IR radiation and the small dipole moment of most molecules prevent the routine application of mid-IR spectroscopy to study nanometer-thick layers. In the mid-IR, a promising alternative to Surface Plasmon Polariton (SPP)-assisted biosensors, widely exploited in the visible range, could be represented by Bloch Surface Wave (BSW)-based biosensors. BSWs are electromagnetic states sustained at the interface between a continuous dielectric medium (in biosensors, this is usually the liquid solution containing the molecules of interest) and a periodic stack of dielectric materials with alternating high/low refractive indices, i.e., a one-dimensional photonic crystal (1DPC) [1]. BSWs are usually excited in a total reflection configuration, hence depositing the 1DPC on the surface of a prism.

The proposed 1DPC consists of a periodic structure of alternating ZnS/CaF_2 layers, both transparent up to 10 μm wavelength (Fig. 1a,b). The 1DPC structure was designed and optimized by means of numerical simulations carried out by the transfer matrix method (TMM) and the multilayers were directly deposited onto CaF_2 prisms by thermal evaporation under high vacuum. The evaporated stack was characterized by slice-and-view with focused ion beam/scanning electron microscopy. Atomic force microscopy and normal-incidence mid-IR reflectance measurements were employed to verify the optical quality of the stack. BSWs spectra were collected in the Kretschmann-Raether configuration by means of a Fourier Transform spectrometer modified so as to produce a quasi-collimated input beam for several different excitation angles θ inside the prism, in order to measure the BSW dispersion (Fig 1c).

We have observed clear spectroscopic evidence of BSWs excitation for both transverse electric (σ) and transverse magnetic (π) polarization in the wavelength range between 3 and 8 μm [2]. At λ=5.6 μm we calculated an evanescent field decay length as short as l_d^{σ} ~810 nm (Fig. 1d), instead of several wavelengths such as in mid-IR SPPs supported by noble metal [2]. More importantly, the nonzero horizontal propagation length of BSWs compared to the simple attenuated total internal reflection (ATR) may increase the interaction length with thin layers. Also, BSW sensors can probe both polarizations, while SPPs can probe only the π polarization. All these features could make BSW biosensors promising candidates for label-free molecule-specific detection of nanometer-thick layers such as antigen-antibody pairs.

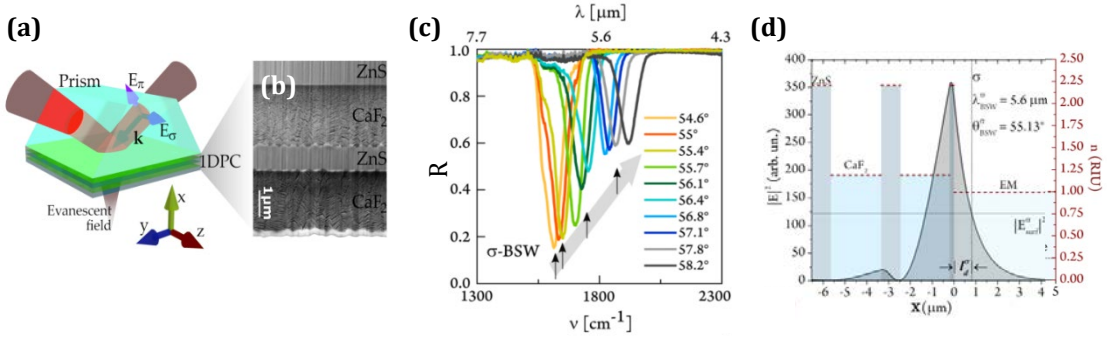

Fig. 1 (a) Pictorial sketch of the 1DPC deposited on the CaF_2 prism. The IR beam impinges on the 1DPC with an incidence angle θ (Kretschmann-Raether configuration). (b) Cross-sectional scanning electron microscopy picture of the 1DPC. (c) BSW spectral features obtained by mid-IR spectroscopy at variable internal reflection angle θ with σ polarized light. (d) Square modulus of the electric field along the direction x perpendicular to the surface. When the incident angle is θ^{σ}_{BSW}= 55.13°, the σ-BSW is excited at 5.6 μm showing a penetration distance l_d^{σ}~810 *nm* and a field enhancement, evaluated as the ratio between the electromagnetic field intensity in the external medium with ($|E_{surf}{}^{\sigma}|^2$) and without ($|E_0|^2$) the 1DPC, of about two orders of magnitude. The dashed red lines indicate the refractive index profile of the 1DPC.

References

[1] Descrovi, E., Sfez, T., Quaglio, M., Brunazzo, D., Dominici, L., Michelotti, F., Herzig, H.P., Martin, O. and Giorgis F. 2010. Nano Lett. 10, 2087–2091.
[2] Occhicone, A., Pea, M., Polito, R.., Giliberti, V., Sinibaldi, A., Mattioli, F., Cibella, S., Notargiacomo, A., Nucara, A., Biagioni, P., Michelotti, F., Ortolani, M. and Baldassarre, L. 2021. ACS Photonics 8 (1), 350-359.

Monitoring Tautomerization of Single Hypericin Molecules in a Tunable Optical $\lambda/2$ Microcavity

Quan Liu[1,2], **Liangxuan Wang**[1,4], **Frank Wackenhut**[1,3], **Marc Brecht**[1,3], **Pierre-Michel Adam**[2], **Johannes Gierschner**[4], **and Alfred J. Meixner**[1]

1 Institute of Physical and Theoretical Chemistry, Eberhard Karls University Tübingen, 72076 Tübingen, Germany.
2 Laboratoire Lumière, Nanomatériaux & Nanotechnologies (L2N), CNRS ERL 7004, Universitéde Technologie de Troyes, 10000 Troyes, France
3 Reutlingen Research Institute, Process Analysis and Technology (PA&T), Reutlingen University, 72762 Reutlingen, Germany
4 Madrid Institute for Advanced Studies, IMDEA in Nanoscience, C/ Faraday 9, Ciudad Universitaria Cantoblanco, 28049 Madrid, Spain.
E-mail: quan.liu@uni-tuebingen.de

Many molecules, such as porphines, porphycenes, or phenanthroperylene quinones, exhibit a reorientation of the transition dipole moment (TDM) during tautomerization. [1] Here, we study single hypericin molecules, which is a prominent phenanthroperylene quinone showing antiviral, antidepressive, and photodynamical properties. [2] Hypericin tautomerization that involves the migration of the labile protons is believed to be the primary photophysical process relevant to its light-activated antiviral activity. Despite the difficulty to isolate individual tautomers, it can be directly observed in single-molecule experiments.

Confocal fluorescence microscopy combined with radially polarized excitation scanning was used to monitor the spatial orientation of TDM of single hypericin molecules in a Poly (vinyl alcohol) matrix. Observing abrupt flipping of the image pattern (as illustrated in Fig. 1) combined with time-dependent density functional theory calculations allows drawing conclusions about the coexistence of four tautomers and their conversion path which are difficult to distinguish in ensemble spectroscopy due to the overlap of the spectra. [3,4] This approach allows the unambiguous assignment of a TDM orientation to a specific tautomer and enables the determination of the chemical structure in situ.

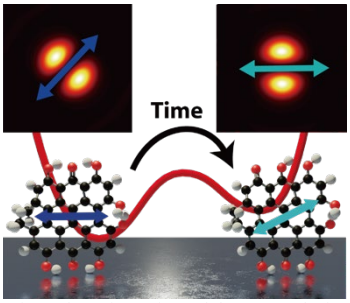

Fig. 1 Illustration of reorientation of the TDM during tautomerization

Moreover, the study can be extended to a λ/2 Fabry–Pérot microcavity. [5] The modification of the local photonic environment by a microcavity is well simulated with a theoretical model that shows good agreement with the experimental data. The excited state lifetime and fluorescence intensity of single hypericin inside a microcavity are correlated, and a distinct jump of the lifetime and fluorescence intensity reveal the temporal behavior of the tautomerization with high sensitivity and high temporal resolution. The observed changes are also consistent with TD-DFT calculations. Our approach paves the way to monitor and even control reactions for a wider range of molecules at the single molecule level.

References

[1] Piatkowski L, Schanbacher C, Wackenhut F, Jamrozik A, Meixner AJ, Waluk J. 2018. *J Phys Chem Lett.* 9(6):1211-1215.
[2] Liu Q, Wackenhut F, Hauler O, et al. 2020. *J Phys Chem A.* 124(12):2497-2504.
[3] Liu Q, Wackenhut F, Wang L, et al. 2021. *J Phys Chem Lett.* 12(3):1025-1031.
[4] Liu Q, Wang L, Roldao JC, et al. 2021. *Advanced Photonics Research.* 2(6):2000170.
[5] Wang L, Liu Q, Wackenhut F, et al. 2022. *J Chem Phys.* 156(1):014203.

Plasmon Enhanced High-Frequency Electron Paramagnetic Resonance - utilization of plasmonic metasurface resonators for magnetic field enhancement at THz frequencies

Martin Hrtoň[1,2], Lorenzo Tesi[3], Peter Kepič[1,2], Katarína Rovenská[1,2], Dominik Bloos[3], Martin Konečný[1,2], Zdeněk Nováček[1,2], Vlastimil Křápek[1,2], Reiner Hillenbrandt[4], A. Leavesly[5], Joris van Slageren[3], and Tomáš. Šikola[1,2]

1. CEITEC BUT, Brno University of Technology, Purkyňova 123, 612 00 Brno, Czech Republic
2. Institute of Physical Engineering, Brno University of Technology, Technická 2, 616 69 Brno, Czech Republic
3 Institute of Physical Chemistry and Center for Integrated Quantum Science and Technology, University of Stuttgart, Pfaffenwaldring 55, 70569 Stuttgart, Germany
4 CICnanoGUNE BRTA and Department of Electricity and Electronics, UPV/EHU, Tolosa Hiribidea 76, 20018 Donostia-San Sebastián, Spain
5 Thomas Keating Ltd., Station Mills, RH14 9SH Billinsgshurst, UK
E-mail: sikola@fme.vutbr.cz

Plasmonic effects, based on localized surface plasmons (LSP) have been used in spectroscopic methods for increasing sensitivity and spatial resolution beyond diffraction limit – one can name Surface-enhanced Raman Spectroscopy (SERS), Tip-enhanced Raman spectroscopies (TERS), Surface-enhanced Infrared Absorption (SEIRA), Plasmon-enhanced fluorescence, etc. In these methods, the electric component of electromagnetic field generated by plasmonic resonant structures (antennas or tips) and its local enhancement are utilized in spectroscopic probes, which corresponds to the fact that this component is in most cases responsible for the interaction with a matter [1]. However, contrary to that, in some methods, for instance in electron paramagnetic resonance (EPR), the magnetic component of electromagnetic radiation is essential [2].

Although, in principle, THz EPR provides high-resolution access to their properties, lack of sensitivity has precluded realizing this potential. To resolve this issue, the plasmonic enhancement of the magnetic component of THz electromagnet near fields by a new type of resonators has been proposed. A resonator composed of an array of diabolo antennas with a back-reflecting mirror was designed and fabricated. Simulations and THz EPR measurements demonstrate a 30-fold signal increase for thin film samples [3]. This enhancement factor increases to a theoretical value of 7500 for samples confined to the active region of the antennas. These findings open the door to the elucidation of fundamental processes in nanoscale samples, including junctions in spintronic devices or biological membranes.

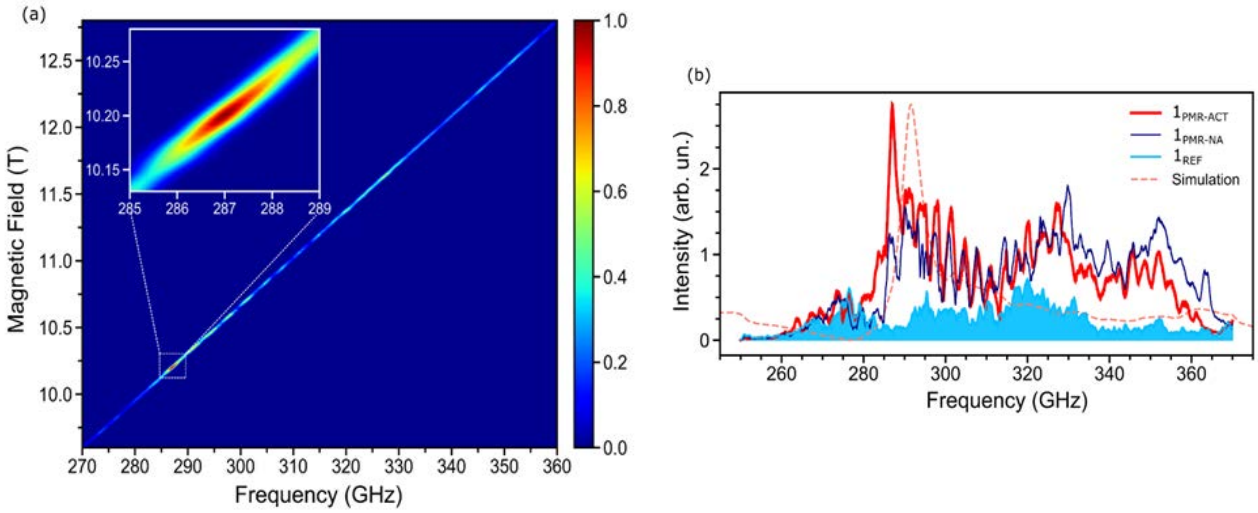

Fig. 1 a) FFMR map measured in HFEPR for 1PMR in the active orientation at 10 K; the PMR resonance area is highlighted in the inset. The colour scale is linear and normalized to unity. b) Comparison of the frequency profiles extracted by the experimental FFMR maps for the PMR in the active (1PMR-ACT), nonactive (1PMR-NA) orientations and for the reference sample constituted by bare quartz (1REF). The simulation of the PMR nearfield intensity is scaled for comparison [3].

References

[1] Mivelle, M; Grosjean, T.; Burr, G.W.; Fischer, U.C.; et al., 2015, ACS Photonics 2, 1071.
[2] Pake, G.E.; Estle, T.L.: The Physical Principles of EPR, W. A. Benjamin, Addison Wesley, Reading, Mass. 1974.
[3] Tesi, L.; Bloos, D.; Hrtoň, M.; Beneš, A.; Hentschel, M.; Kern, M.; Leavesley, A.; Hillenbrand, R.; Křápek, V.; Šikola, T.; and van Slageren, J., Small Methods 2021, 5, 210037.

AFM-TERS measurements in liquid environment with side illumination/collection

Patrick Hsia[1], **Pierre Burgos**[2], **Marc Chaigneau**[1]

1. HORIBA France SAS, 14, Bd. Thomas Gobert - Passage Jobin Yvon CS 45002 - 91120 Palaiseau - France
2. HORIBA UK Ltd., Kyoto Cl, Moulton Park Industrial Estate, Northampton NN3 6FL - UK
E-mail: patrick.hsia@horiba.com

The new breakthrough in Raman nanoscale chemical imaging is the measurement in liquid environment. TERS measurements in liquid will significantly broaden the potential application of TERS across scientific disciplines such as heterogeneous catalysis[1,2], electrochemistry[3,4], cellular biology [5], and biomaterials [6]. Implementation of TERS in liquid brings out some instrumental difficulties. AFM-TERS in liquid have been published quite recently but mainly in bottom [7], and top [6], optical accesses.

In this talk, specifics of the TERS setup that enables measurements in liquid with side illumination/collection in order to keep optimal polarization conditions will be discussed: the design of a side access liquid cell that allows high-throughput optics, the possibility to perform AFM imaging in true non-contact mode in liquid, the alignment procedure of the Raman laser to the AFM-TERS tip in liquid using objective scanner (Fig. 1).

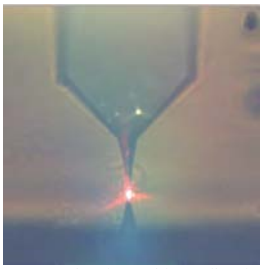

Fig. 1 Laser pre-aligned on the tip in liquid environment. The tip and its reflection on the substrate can both be seen on this picture

Thanks to those latest instrumental developments, we will present the nanoscale imaging in liquid of graphene oxide and carbon nanotubes immersed in water. TERS resolution in liquid down to 20 nm is demonstrated along with true non-contact AFM images (Fig. 2).

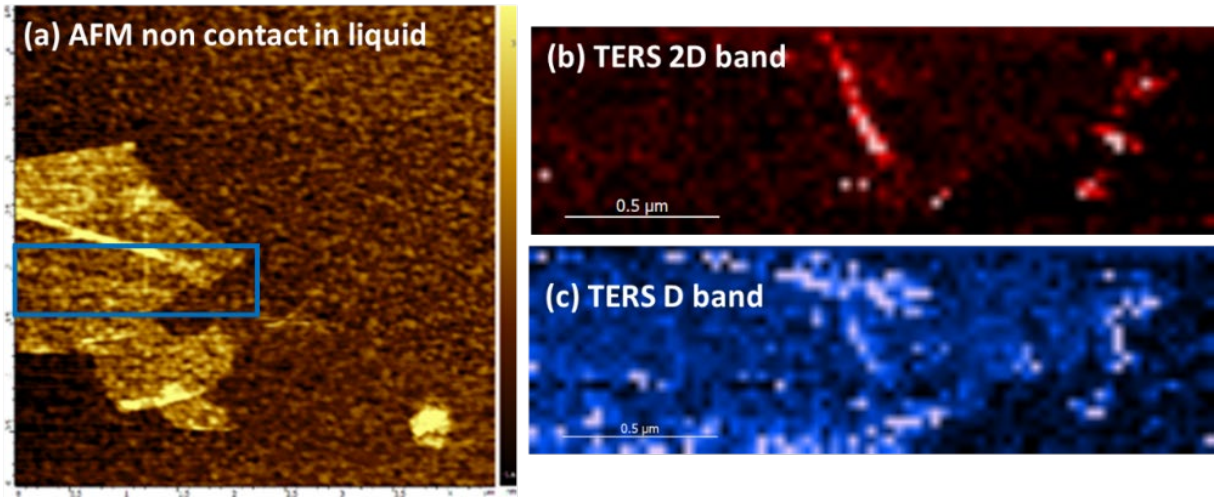

Fig. 2 (a) AFM imaging (true non-contact mode) of graphene oxide flake in liquid, (b) TERS map of the 2D band and (c) TERS map of the D band.

References

[1] Li, Z. et al., 2021, *Chem. Commun.*, 57, 891-894
[2] Cai, Z.-F. et al., 2021, *J. Am. Chem. Soc.*, 144, 538-546
[3] Touzalin, T. et al., 2019, *Electrochem. Commun.*, 108, 106557
[4] Huang, S.-C. et al., 2019, *Anal. Chem.*, 91, 11092-11097
[5] Lipiec, E. et al., 2014, *Angew. Chem. Int. Ed.*, 53, 169-172
[6] Lipiec, E. et al., 2021, *Angew. Chem. Int. Ed.*, 60, 4545-4550
[7] Bhattarai, A. et al., 2019, *J. Phys. Chem. C*, 123, 7376-7380

Molecular Stark Effect at the Nanoscale

Demelza Wright[1†], **Sara Sangtarash**[2], **Niclas S. Mueller**[1], **Qianqi Lin**[1], **Hatef Sadeghi**[2], **Jeremy J. Baumberg**[1]

1. NanoPhotonics Centre, Department of Physics, Cavendish Laboratory, University of Cambridge, Cambridge, UK.
2. Device Modelling Group, School of Engineering, University of Warwick, Coventry, UK
E-mail: daw85@cam.ac.uk

Sensing local electric field is important to gain insights into catalysis, biomolecular binding (e.g., in medical devices), or in molecular electronics. The smallest field sensor is a single polar chemical bond, whose vibrational resonance shifts in electric fields and is known as a Stark probe. Here, we show for the first time how ionic double layers can sometimes penetrate molecular layers, and how this can be measured and controlled.

Molecular self-assembled monolayers (SAMs) support polar bonds for sensing. However, little is understood about charge transport or ionic movement within SAMs because direct measurements are extremely challenging. We find here that ions are excluded from SAMs by surrounding phenyl groups, preventing the formation of a penetrating electrical double layer and thus directly modifying the local field on the nanoscale. This has important consequences for driving-force sensitive surface reactions taking place in mixed, multi-molecular, or 'dirty' environments.[1]

Plasmonic nanogaps using the NanoParticle-on-Mirror (NPoM) geometry enhance Raman intensities by 10^8, facilitating high signal-to-noise spectroscopy of only a few hundred molecules and significantly increasing spectral quality by minimizing averaging effects.[2] Our previous work utilized this to perform a mechanistic analysis of molecular catalysts: revealing the first direct evidence of an intermediate state involving a thiol linker.[3] Co-opting this approach, we now address a topic with little agreement in literature: the interaction of the electrical double layer and SAMs. We combine theoretical and experimental approaches in tracking multiple vibrational modes of a SAM with a C≡N Stark reporter group moiety in response to electrochemical fields (Fig.1a**)**.[4]

We observe Stark shifts in multiple vibrational modes that cannot be described by the commonly used linear-field density functional theory model. Instead, we show that modelling the movement of a single local ion close to the C≡N group describes the results well, with ion movement of only 2 Å accounting for most vibrational changes. By sterically hindering ions from accessing the C≡N group using a mixed SAM system with a larger biphenyl molecule (Fig.1b**)** we observe strong impacts on the Stark shifts. We fully suppress Stark shifting in heavily diluted mixtures and decrease the Stark effect for intermediate mixtures (Fig.1c**)**, supporting our conclusion that stacking of phenyl groups prevents electrical double layer formation within SAM layers. We thus identify and control the position of the electrical double layer at a SAM interface.

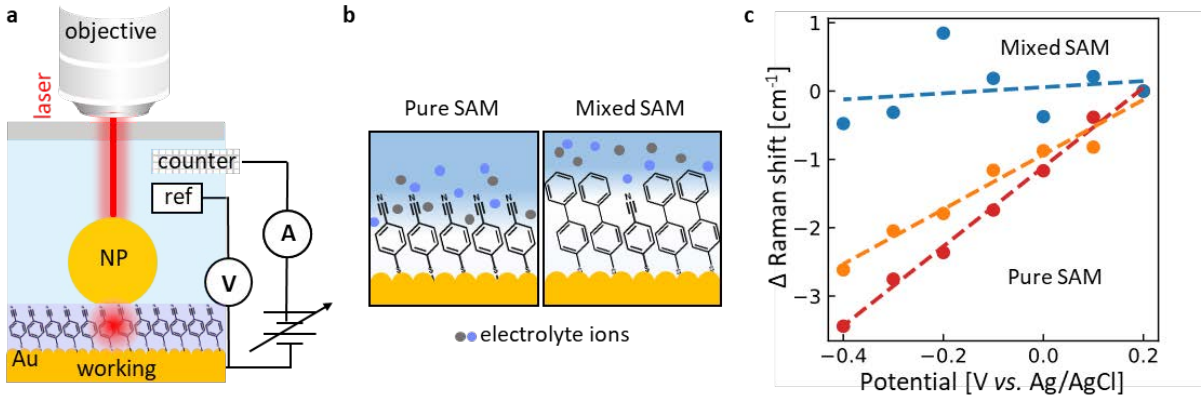

Fig. 1 a. Electrochemical nanogap spectroscopy from single plasmonic junctions. **b**. Schematic of ion movement near pure and mixed self-assembled monolayers. **c**. Molecular Stark shifting in pure and mixed self-assembled monolayers.

† Present address: Department of Electrical and Computer Engineering, University of Victoria, Victoria, British Columbia, Canada

References

[1] Moore, E.E.; Cobb, S.J.; Coito, A.M.; Oliveira, A.R.; Pereira, I.A.C.; Reisner, E. 2022, *PNAS* **119**, e2114097119.
[2] Kamp, M.; de Nijs, B.; Kongsuwan, N.; Saba, M.; Chikkaraddy, R.; Readman, C.A.; Deacon, W.M.; Griffiths, J.; Barrow, S.J.; Ojambati, O.S.; Wright, D.; Huang,J.; Hess, O.; Scherman, O.A.; Baumberg, J.J. 2020, *PNAS* **117**, 14819
[3] Wright, D.; Lin, Q.; Berta, D.; Földes, T.; Wagner, A.; Griffiths, J.; Readman, C., Rosta, E.; Reisner, E.; Baumberg, J.J. 2021, *Nat Catal*, **4**, 157.
[4] Wright, D.; Sangtarash, S.; Mueller, N.S.; Lin, Q.; Sadeghi, H.; Baumberg, J.J.; submitted (2022)

Terahertz Spoof Surface Plasmon Polariton sensor on thin Silicon-Nitride membrane

Mohsen Haghighat[1], **Levi Smith**[1], **Thomas Darcie**[1]

1. Department of Electrical and Computer Engineering, University of Victoria, Victoria, BC V8P 5C2, Canada

E-mail: mohsenh@uvic.ca

Our Terahertz System-On-Chip (TSoC) enables high-speed baseband pulse transmission along with low-loss and low-dispersion by creating circuits on a thin (1 μm) Silicon Nitride membrane [1]. Spoof surface plasmon polariton (SSPP) waveguides are candidates to enable miniaturized terahertz integrated circuits and systems [2]. Tapered SSPP structures have been used for focusing or channeling terahertz radiation to micron-scale volumes for near-field imaging, spectroscopy, and sensing applications [3]. Previous work related to this application has used a conical structure [3]. Here we focus on a planar on-chip integration using a Goubau line [4]. We use an open-circuited line to create a high-intensity field at the tip of a tapered Goubau line.

In this work, we simulate a tapered and corrugated SSPP device integrated onto our experimentally compatible TSoC platform for THz focusing. Fig. 1 shows the electric field magnitude of simulated Tapered SSPP at three different frequencies (e.g., 0.25, 0.50, and 0.75 THz). The simulation is used by the commercial finite element method (FEM) solver ANSYS HFSS, and a terminal solution with a single wave port is used to simulate the structure. The conductor is Gold (Au) with 200nm thickness on a 1 μm Silicon-Nitride substrate with a length and width of 2mm. The length waveguide is 0.5mm shorter (e.g., 1.5mm) to observe the focusing on the surface of metal and dielectric. By integrating a tapered SSPP Goubau transmission line we can increase the local field intensity at the tip by more than 15dB from 0.1 to 1 THz. The reflection magnitude intensity changes in the presence of different chemicals, and it can be optimized based on a particular analyte.

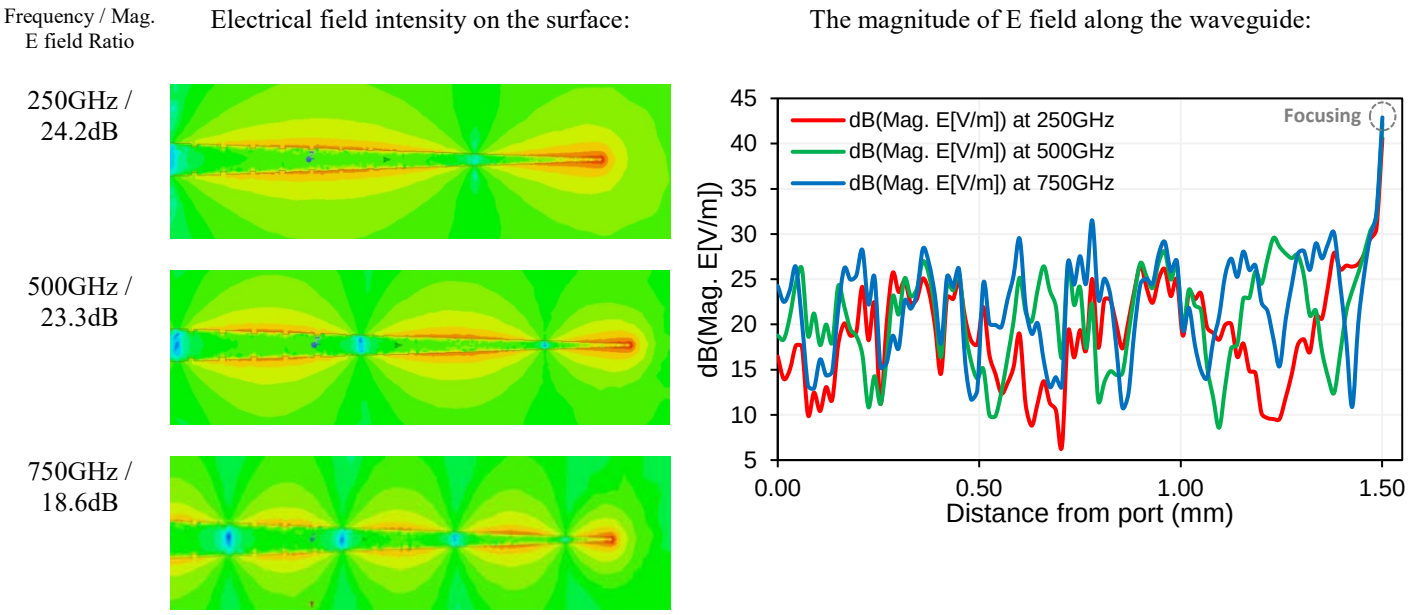

Fig. 1. The simulation of the planar tapered SSPP Goubau line on Si_3N_4 membrane for THz focusing and Magnitude of Electric field (in dB Scale) along the waveguide

References

[1] L. Smith, V. Shiran, W. Gomaa, and T. Darcie, 2021, "Characterization of a split-ring-resonator-loaded transmission line at terahertz frequencies," *Opt. Express* 29, 23282-23289.

[2] M. A. Unutmaz and M. Unlu, 2019 "Terahertz Spoof Surface Plasmon Polariton Waveguides: A Comprehensive Model with Experimental Verification," *Scientific Reports*, vol. 9, no. 1, p. 7616

[3] S. A. Maier, S. R. Andrews, L. Martín-Moreno, and F. J. García-Vidal, 2006, "Terahertz Surface Plasmon-Polariton Propagation and Focusing on Periodically Corrugated Metal Wires,", 2006, *Phys. Rev. Lett.*, vol. 97, no. 17, p. 176805.

[4] T. Akalin, A. Treizebre and B. Bocquet, "Single-wire transmission lines at terahertz frequencies,", 2006, *IEEE TMTT*, vol. 54, no. 6, pp. 2762-2767.

Evaluation of SERS substrates through average and high fluctuation regimes

Arash Azarakhshi[1], **Alexandre G. Brolo**[2]

1. Department of Physics and astronomy, University of Victoria, Victoria BC Canada
2. Department of Chemistry, University of Victoria, Victoria BC Canada
E-mail: agbrolo@uvic.ca

Surface-Enhanced Raman scattering (SERS) is a well-known phenomenon that provides an increment of up to 10^{10} in the number of Raman scattered photons.[1] SERS is achieved through the excitation of surface plasmon polaritons (SPP's) at the surface of metal nanoparticles/nanostructures leading to highly concentrated local electrical field hotspots (HS) beyond the diffraction limit.[2] Presence of a probe molecule inside of a strong HS results in a SERS signal which could pass the instrumental detection threshold. While the enhancement factor (EF) is the most common parameter to report the quality of the SERS substrates,[3] but the broad ranges of definitions, experimental and theoretical procedures and the lack of a temporal and spatial resolution make this parameter an unreliable factor. Providing the universal standards to evaluate and compare different SERS substrates based on the temporal and spatial variations of the SERS signals is the central pursuit of our work. Though evaluation of the signal in the average SERS regime would provide useful insight toward the quality of the substrate, we also implement the high fluctuation regime to relate the signal characteristics to physical features of the HSs either density or strength. As shown in Fig.1, for the average SERS regime the signal fluctuates symmetrically around the mean value with the small Mean Absolute Deviation (MAD) while in the high fluctuation regime SERS signal could fluctuate further from the mean value which would lead to higher MAD.

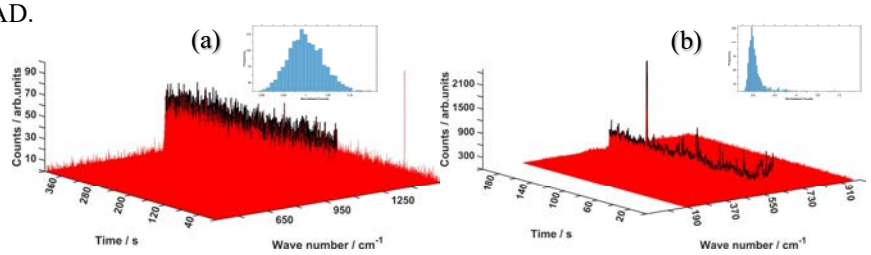

Fig1. Temporal fluctuation of the SERS signal obtained from the same substrate for two different regimes. **a.** 1mMPyridine, **b.** 50 nM Nile Blue

Fig.2 implies the evaluation parameters and results for two commercial gold substrates in both average and high fluctuation SERS regimes. Additionally, we collect data in the solution phase to benefit from the dynamic variation of the signal.

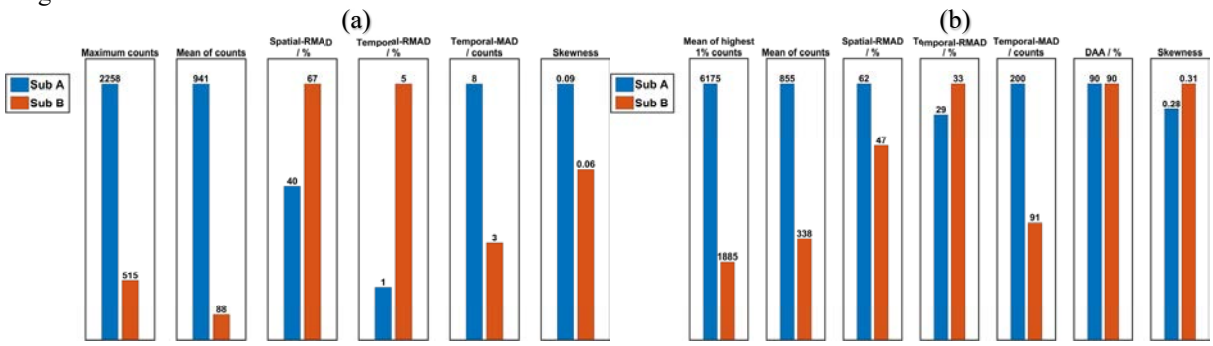

Fig2. Evaluation Parameters of the SERS substrate. **a.** Average SERS regime, **b.** High fluctuation regime

According to Fig.2, substrate A demonstrates higher temporal fluctuations but its stronger signal leads to a smaller RMAD. The higher mean and maximum intensity from Substrate A could root from different possible scenarios: higher density of HSs, possession of stronger HSs, or both. To link the behavior of substrates to their physical properties we move to the high fluctuation regime which reveals that the Density of Active Area (DAA)-the fraction of nonzero events- for both substrates are similar, however, substrate B still produces higher counts. Thus the better performance of Substrate A arises from the stronger HSs rather than a higher density of HSs. Consequently, our analysis directs how to employ the various evaluation parameters in different regimes to evaluate and compare the SERS substrates.

References

[1] Ru, E. C. L.; Blackie, E.; Meyer, M.; Etchegoin, P. G. 61. SERS A Comprehensive Study. 2007, 13794 13803.

[2] Willets, K. A. Super-resolution imaging of SERS hot spots. Chemical Society Reviews 2014, 43, 3854 3864.

[3] Rodrigues, D. C.; De Souza, M. L.; Souza, K. S.; Dos Santos, D. P.; Andrade, G. F.; Temperini, M. L. Critical assessment of enhancement factor measurements in surface enhanced Raman scattering on different substrates. Physical Chemistry Chemical Physics 2015, 17, 21294 21301.

Monitoring metabolic alterations in cancer cells upon radiotherapy by SERS

Xiangyu Chen[1], **Javier Plou**[2]

1. University of Victoria, 3800 Finnerty Road, Victoria, BC, Canada
2. CIC biomaGUNE, Basque Research and Technology Alliance (BRTA), 20014 Donostia-San Sebastián, Spain.
E-mail: xiangyuchen@uvic.ca

Abstract: Surface-enhanced Raman scattering (SERS) spectroscopy has been recognized as a promising technology for biomedical analysis and clinical diagnosis thanks to its high sensitivity and label-free operation. As a real-time probe of the exogenous metabolites of cells, SERS exhibits simpler, faster, and less expensive advantages. The tumor microenvironment (TME) is a very complex cellular ecosystem characterized by an altered metabolism. Analysis of the SERS spectra of the metabolisms from breast cancer cells allows the identification of characteristic patterns in the extracellular environment of breast cancer cells before and after radiotherapy treatment. The release of specific metabolites from cells that have resisted radiotherapy treatment may have significant implications in tumor recurrence after therapy. Here, we fabricated the plasmonic substrates based on silver nanoparticles enhancing the Raman signal of metabolites from the cell supernatant and performing irradiation of cells with different irradiation doses (Gy5 and Gy20). The recorded SERS spectra from the extracellular environment after 2-week of radiotherapy exhibit meaningful differences between control and irradiated cells (see **Fig.1**).

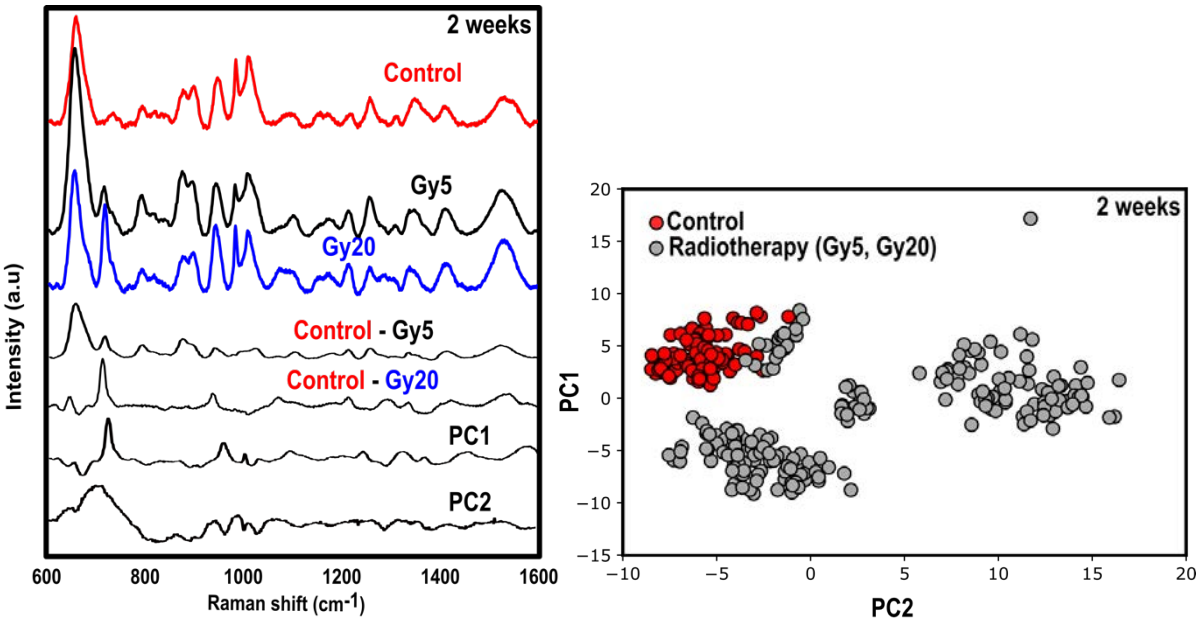

Fig. 1 SERS spectra (left) and Two-Dimensional Principal Component Analysis (right) of extracellular environment of breast cancer before treatment and after 2 weeks of treatment

Unveiling the role of chemical and electronic structure in plasmon catalysis using alkoxyamines as a chemical probe

Darya Votkina,[1] Pavel Petunin, [1] Andrii Trelin, [2] Oleksiy Lyutakov,[2] Gérard Audran,[3] Rashid Valiev,[4,5] Sylvain R. A. Marque,[3] and Pavel Postnikov,[1,2] Yusuke Yamauchi[6], Olga Guselnikova[1]

1 Research School of Chemistry and Applied Biomedical Sciences, Tomsk Polytechnic University, Russian Federation.
2 Department of Solid-State Engineering, University of Chemistry and Technology, Prague, Czech Republic.
3. Aix-Marseille Univ, CNRS, ICR case 551, Avenue Escadrille Normandie-Niemen, 13397 Marseille Cedex 20, France
4. Tomsk State University, 36, Lenin Avenue, 634050 Tomsk, Russia.
5. University of Helsinki, Department of Chemistry, P.O. Box 55, (A.I. Virtanens plats 1), FIN-00014 University of Helsinki, Finland
6. JST-ERATO Yamauchi Materials Space-Tectonics Project, International Center for Materials Nanoarchitectonics (WPI-MANA), National Institute for Materials Science, 1-1 Namiki, Tsukuba, Ibaraki, Japan

guselnikova.olga@nims.go.jp

The excitation of localized plasmon resonance on nanoparticles followed by the interaction with organic molecules leads to new pathways of chemical reactions [1]. Although a number of physical factors (temperature, illumination regime, type of nanoparticles, etc.) are affecting this process, the role of the chemical factors is underestimated [2, 3, 4, 5]. Challenging this assumption, here we studied the kinetic of plasmon-induced homolysis of five alkoxyamines (AAs) with different chemical and electronic structures using electron paramagnetic resonance (EPR) (Fig. 1).

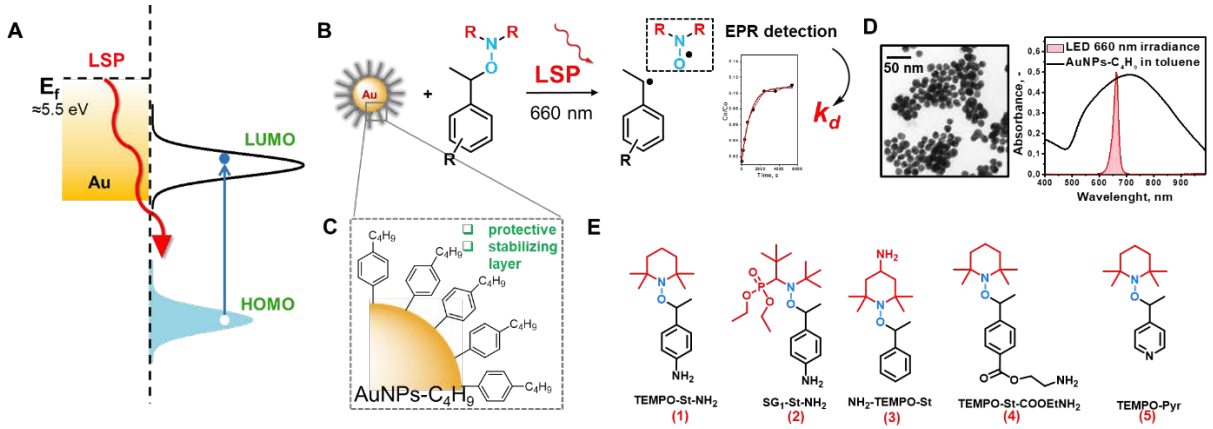

Fig. 1. Overview of the experimental strategy. **A** - Scheme for the direct intramolecular excitation mechanism via localized surface plasmon (LSP) resonance and location of HOMO, LUMO levels, **B** - Scheme of plasmon-induced homolysis of alkoxyamines using AuNPs-C_4H_9, **C** - the structure of organic layer, **D** -TEM image, and UV-Vis spectra of AuNPs-C_4H_9, E- structures of alkoxyamines investigated.

The kinetic data revealed the dependence of plasmonic homolysis rate constant (kd) with the HOMO energy of AAs, which cannot be described by the kinetic parameters derived from thermal homolysis experiments. The observed trend in kd allowed to suggest the key role of intramolecular excitation mechanism supported by the DFT calculations, additional spectroscopic characterization, and control experiments. This observation suggests that the electronic structure of organic molecules may play a key role in other related reactions in plasmon catalysis

References

[1] Zhang Z., Zhang C., Zheng H. and Xu, H. *2019,* Acc. Ahem. Res., 52, 2506–2515.
[2] Guselnikova O., Váňa, J., Phuong, P., Panov, I., Rulíšek, L., Trelin, A., Postnikov, P., Švorčík, V., Andris, E. Lyutakov, O. *2021,* Chem. Sci., 12, 5591–5598.
[3] Olshtrem, A., Guselnikova, O., Postnikov, P., Trelin, A., Yusubov, M., Kalachyova, Y., Lapcak, L., Cieslar, M., Ulbrich, P., Svorcik, V., Lyutakov, O., *2020*, Nanoscale, 12, 14581–14588.
[4] Ezina, M., Guselnikova, O., Miliutina, E., Trelin, A., Postnikov, P., Svorcik, V., Lyutakov, O., *2021*, J. Phys. Chem. C, 125, 10318–10325.
[5] Guselnikova, O., Audran, G., Joly, J.-P., Trelin, A., Tretyakov, E., Svorcik, V., Lyutakov, O., Marque, S. R. S., Postnikov, P., *2021*, Chem. Sci., 12, 4154–4161.

Near Infrared Waveguide using multilayer ITO metamaterial

Shashwata Chattopadhyay and J Mitra

School of Physics, Indian Institute of Science Education and Research Thiruvananthapuram, kerala (695551), INDIA.

E-mail: shash00817@iisertvm.ac.in

Optical waveguides of subwavelength dimensions, for enabling on-chip all optical or electro-optic modulation has remained a challenge in terms of efficient light coupling with low propagation losses. Epsilon near zero (ENZ) materials like indium tin oxide (ITO) offer multiple advantages for realizing such a on-chip device. Transparent in the visible ITO undergoes a dielectric to metal transition at the ENZ wavelength, at which the real part of its dielectric constant (Re(ϵ)) becomes zero[1]. The near zero relative permittivity and refractive index below 1 nucleates interesting optical properties therein like perfect absorption (PA)[2], local electric field enhancement and high nonlinearities[3]. In parallel the conducting nature of the oxide allows for electro-optic modulation where the refractive index of the material may be modulated by an applied voltage. Here we propose a sandwich waveguide structure of stacked ITO multilayers on glass substrate, with a low electron density ITO (n=1e27 m^{-3}) having ENZ wavelength 2.22 µm of thickness 10 nm in between two higher electron density ITO (n=2e27 m^{-3}) having ENZ wavelength 1.52 µm of thickness 50 nm and 90 nm respectively. In the attenuated total internal reflection (ATR) configuration this stack allows for exciting modes in the middle ITO waveguide in wavelength regimes where the stack behaves as a metallic-dielectric-metallic metamaterial.

Finite element modelling simulations performed on the above structure shows feasibility of efficient light coupling into the waveguide in the spectral range 1.7 - 2.1 µm. Figure 1a shows the effective dielectric constant of the sandwich waveguide showing a protracted spectral region with Re(ϵ) close to zero. Figure 1b plots the y-component of the Poynting vector quantifying the energy transport along the dielectric ITO channel in an analogous ITO waveguide where the third ITO layer is replaced by 40 nm of Au, for incident excitation of 1.88 µm. Figure 1c then shows the variation of the Poynting vector along the dashed line in figure 1b showing the energy localization within the 10 nm waveguide. Across the applicable spectral window our results show that approximately 1/3rd of the incident power is successfully coupled into the proposed waveguide using a simple stacked multilayer of ITO. We further discuss experimental realisation of the waveguide and electro-optic modulation of the same by application of bias across the ITO channel.

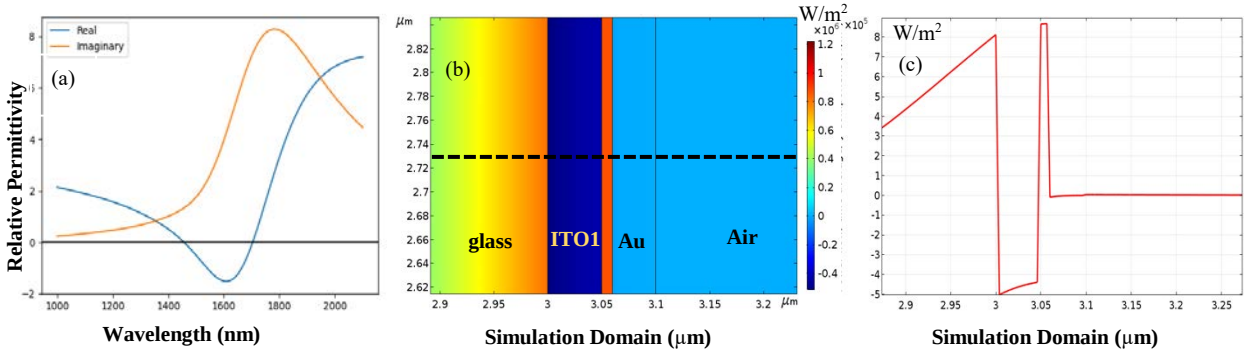

Fig. 1 (a) Effective relative permittivity vs wavelength of the stacked multilayer ITO. **(b)** Y-Component of Poynting's vector mapped across the simulation model domain with ITO1 (n=1e27 m^{-3})-ITO2 (n=2e27 m^{-3})-Au **(c)** Y-Component of Poynting's vector along the dashed line in figure 1(b).

References

[1] Johns, B., Puthoor, N. M., Gopalakrishnan, H., Mishra, A., Pant, R., & Mitra, J. *2020*. Epsilon-near-zero response in indium tin oxide thin films: Octave span tuning and IR plasmonics. *Journal of Applied Physics*, *127*(4).

[2] Johns,Ben Chattopadhyay,Shashwata Mitra,Joy ,*2022*, Advanced Photonics Research, Volume 3, Issue 1, 2100153.

[3] Suresh, S., Reshef, O., Alam, M. Z., Upham, J., Karimi, M., & Boyd, R. W. *2021*. Enhanced Nonlinear Optical Responses of Layered Epsilon-near-Zero Metamaterials at Visible Frequencies. *ACS Photonics*, *8*(1), 125–129.

Creation of wide stopbands by loading split-ring-resonators to a terahertz guided-wave coplanar strip transmission line

Saeid Asadi[1], **Levi Smith**,[1] **Thomas Darcie**[1]

1. Department of Electrical and Computer Engineering, University of Victoria, BC, V8W, Canada

saeid.asadi86@gmail.com, levismith@uvic.ca, tdarcie@ece.uvic.ca

In this paper, split-ring-resonator (SRR) meta-atoms (metamaterials) are placed between the two conductors of a coplanar strip (CPS) THz transmission line (TL). This CPS TL is designed on a thin (1μm) Silicon Nitride membrane which enables operation up-to 3 THz. Adding a SRR in a TL introduces a resonance corresponding to a negative permeability ($\mu < 0$) [1] which appears as a stopband [2]. In the previous work [3], equal sized meta-atoms are placed near a guided-wave CPS TL which led to a single resonance and narrow stopband. In this work, we widen the stopband by varying the radius of each meta-atom. This study has been performed by the ABCD matrix approach [4].

Fig. 1(a) illustrates a CPS TL loaded with a single SRR. In Figs. 1(b, c), obtained by simulation (HFSS), the electric field intensity is observed off and on resonance, respectively. Modifying the radius of a SRR changes its resonant frequencies. In Fig. 2, the TL containing one SRR is compared with TL containing three and four SRRs in terms of the S_{21} parameter. In Fig. 2(a), all the SRRs have the same radius in both configurations; however, the TL with three SRRs has a wider stopband. In Fig. 2 (b), the radii of SRRs, of the TL with three SRRs, are changed which corresponds to a variation in the equivalent inductance and capacitance and a wide stopband (about 0.1 THz). Therefore, by adding more SRRs, not only is it possible to further widen the stopband and thus the region where $\mu < 0$, also we can further weaken components in the stopband as depicted in Fig. 2 (c) which the TL contains four different radii SRRs.

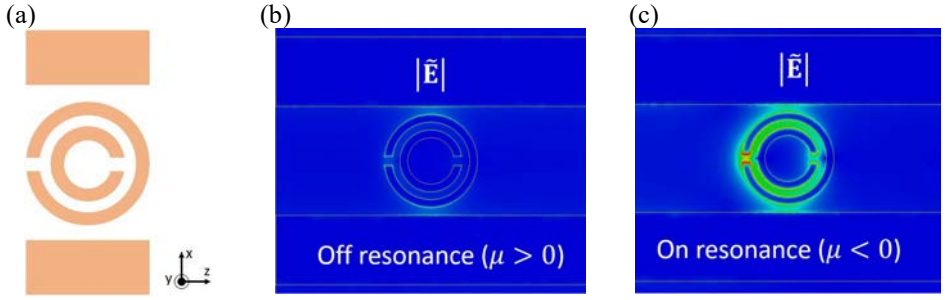

Fig. 1. (a) CPS TL containing a single SRR. (b) and (c) Electric field pattern in off and on resonance, respectively.

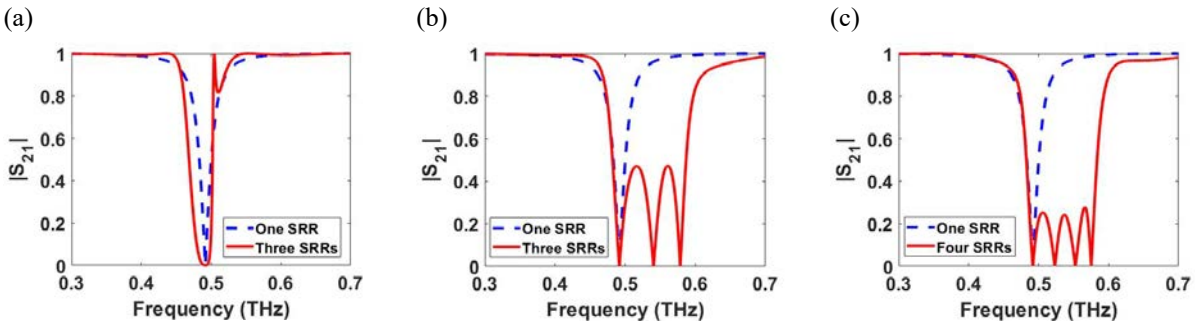

Fig. 2. S_{21} parameter of CPS TL containing SRRs. The dashed line characterizes a TL containing one SRR. The solid line characterizes a TL including three and four SRRs. (a) All the SRRs have equal radii. (b) The three SRRs have different radii. (c) Four SRRs with different radii.

References

[1] Pendry, J, B. Holden, A, J. Robbins, D, J. Stewart, W, J. 1999. *IEEE Transactions on Microwave Theory and Techniques*, 47, 2075-2084.
[2] Syms, R, R, A. Shamonina, E. Kalinin, V. Solymar, L. 2005. *J. Appl. Phys*, 97, 064909.
[3] Smith, L. Shiran, V. Gomaa, W. Darcie, T. 2021. *Optics Express,* 29, 15-19.
[4] Pozar, D, M. Microwave Network Analysis, *Microwave Engineering*. 2012, John Wiley & Sons, Inc, United States, 188-194.

Broadband absorber utilizing nonlocal metamaterials

Won-Heum Han[1], **Q-Han Park**[2]

1,2 Korea University/Nanooptics lab, 145 Anam-ro, Seongbuk-gu, Seoul, 02841, Rep. of Korea.

E-mail: hanwh.mail@gmail.com[1], qpark@korea.ac.kr[2]

Electromagnetic wave absorbers are widely used for various applications including stealth technology and minimizing EM wave interference between automobile electronic components. There are many previous studies especially in the X-band(8-12GHz) region to design an absorber attached to PEC with design methods such as the frequency selective surface(FSS) [2], metamaterial and multilayer methods[3]. In the case of the FSS study, the absorption performance reaches about -15dB reflectance (lower reflectance refers to better absorption performance). Reflectance below -20dB has been reported when either TE or TM polarization has been specifically selected. In the multi-layer case aimed for a broadband operation, the thickness of an absorber has to increase significantly to assure the absorption performance. Earlier studies have shown a -10dB reflectance with thickness 3.04mm and -20dB with thickness 10mm. For practical applications, it is highly desirable to design a thin X-band absorber with reflectance less than -20dB covering all polarizations and broadband.

To achieve the high absorption performance with ultrabroadband operation, nonlocal absorbers enabling the universal impedance matching(UIM) have been suggested[1]. In this study, we present a nonlocal metamaterial absorber which was designed to meet the UIM condition approximately. A broadband absorber is made of silicone rubber with an embedded double layered conductive wire. Wires of each layer contains a resistor, marked in cyan color in Fig. 1(a). The overall thickness of an absorber is about a quaterwavelength while the size of an unit is also of subwavelenth scale. Full wave numerical calculations shows a good performance with results on the reflectance in the X-band of the proposed structure illustrated in Fig.1 (b). We achieve a reflectance less than -20dB which is smaller when compared to other studies of similar thickness. Other additional strengths of our work are summarized in the Table 1 with comparisons to previous studies.

	Reflectance	TE, TM cover	Thickness	Number of materials	Flexibility
FSS method[2]	-15dB	some possible	3~7mm	2~3	X
Multilayer[3]	-10dB	possible	3mm~	3~5	X
This study	-20dB	possible	4mm	3	O

Table. 1 Comparison Analysis of X-band Absorbers.

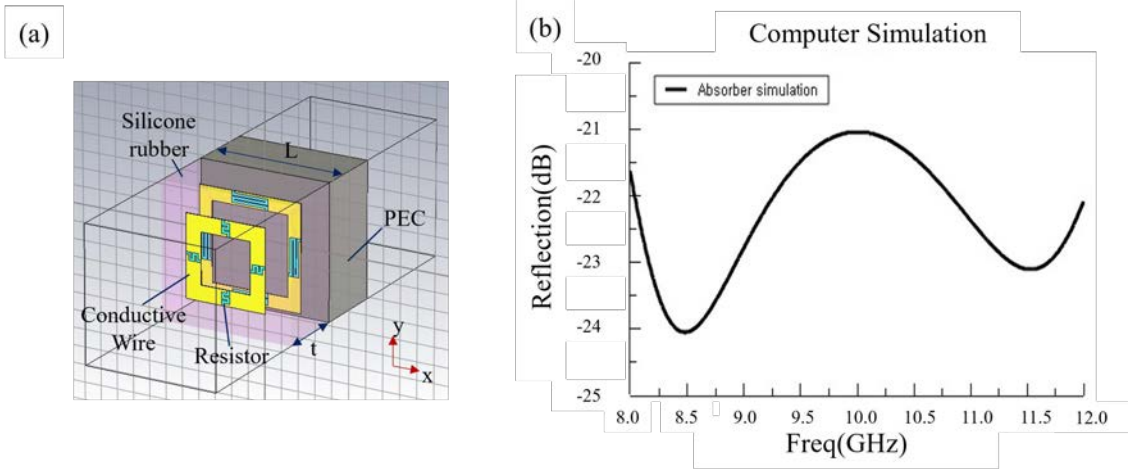

Fig. 1 (a) CST modeling. (b) Simulation result

References

[1] Im K, Kang JH and Park QH. 2018. Nature Photon 12, 143-149.
[2] Sohrab A P, Atlasbaf Z. 2013. IEEE Antennas and Wireless Propagation Letters, vol. 12, 276-279
[3] Choi WH, Shin JH, Song TH, Kim JB, Lee WY, Kim CG. 2015 Composite Structures Volume 124, 310-316

NFO16
FIB defined curved architectures toward asymmetric chiral metasurfaces

Ruhao Pan[1], **Changzhi Gu**[1*], **Junjie Li**[1*]

Beijing National Laboratory for Condensed Matter Physics, Institute of Physics, Chinese Academy of Sciences, Beijing 100190, China
E-mail: panruhao@iphy.ac.cn

3D chiral metasurfaces show great advantages in modulating the spin-states of the electromagnetic waves, and thus give crucial opportunities to next-generation bio-sensors and optical communication devices[1,2]. However, the lack of arbitrary structure controls and giant CDs hinders the application of 3D metasurface.

Here, we have developed a focused ion beam (FIB) defined origami method, which can generate 3D curved configurations in micro/nano-scale by FIB global irradiation of the planar cantilevers, showing great potential in the realization of multifunctional metasurface that can hardly be achieved by 2D patterns. The curved deformation during the FIB irradiation comes from the tensile stress that induced by the ion-matter interaction. As shown in **Fig.1**, by simultaneously modulating the cantilevers' patterns and FIB irradiation parameters, the curved 3D architectures with controllable shapes and curvature down to 175 nm are taken shaped over a large scale.

A chiral metasurface consisting of curved asymmetric split ring resonators (SRR) with intrinsic chirality is designed and shown in F**ig.2**. Because the curved arm of the SRR breaks the symmetry in z-space, the chiral metasurface shows asymmetric chirality for the light illuminate from different directions. Greater CDs at 5.2 μm can be observed for the backward incident compared to the forward incident. The CDs change with the curved angle of the metasurface, and metasurface with 60° curved angle show highest CD of 0.85/0.71 by simulation/experiment for backward beam incidence, while the CD is shrunk to -0.29/-0.29 for forward incidence. The near-filed distribution shows the asymmetric chirality comes from the electronic and magnetic dipoles are neither parallel nor vertical, which results in that $\vec{p} \cdot \vec{m} \neq 0$ and $|\vec{p} \times \vec{m}| \neq 0$.

FIB defined origami not only shows a new method to build up 3D metasurfaces with asymmetric chirality, but also inspiring a new approach to designing multifunctional and high efficiency photonic devices.

Fig. 1 Diverse curved structures fabricated by FIB defined origami method

Fig.2 The SEM image and the optical properties of the asymmetric chiral metasurface

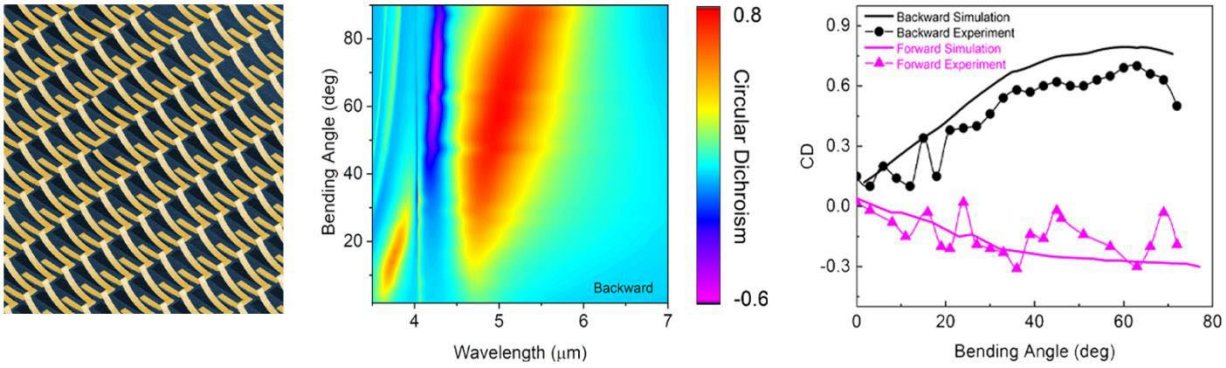

References

[1] Liang, Y; Lin, H; Koshelev, K,; et al. 2021. *Nano Lett.*, 21, 1090-1095.
[2]Wang C; Li, Z; Pan, R; et al. 2020. *ACS Photonics*, 7, 3415-3422.

Infrared Near-Field Spectroscopy at the National Synchrotron Light Source II

Lukas Wehmeier[1], **Ziheng Yao**[2], **Mengkun Liu**[1,2], **and G. Lawrence Carr**[1]

1. National Synchrotron Light Source II, Brookhaven National Laboratory, Upton, New York 11973, USA
2. Department of Physics and Astronomy, Stony Brook University, Stony Brook, New York 11794, USA
E-mail: lwehmeier@bnl.gov

Infrared near-field spectroscopy provides unique capabilities for exploration of the nanoworld as it combines the information density of optical techniques with the spatial resolution of atomic force microscopy of ~10 nm. Despite rapid technological development in the past decades, the availability of suitable table-top laser sources still severely limits the accessible infrared spectral range [1].

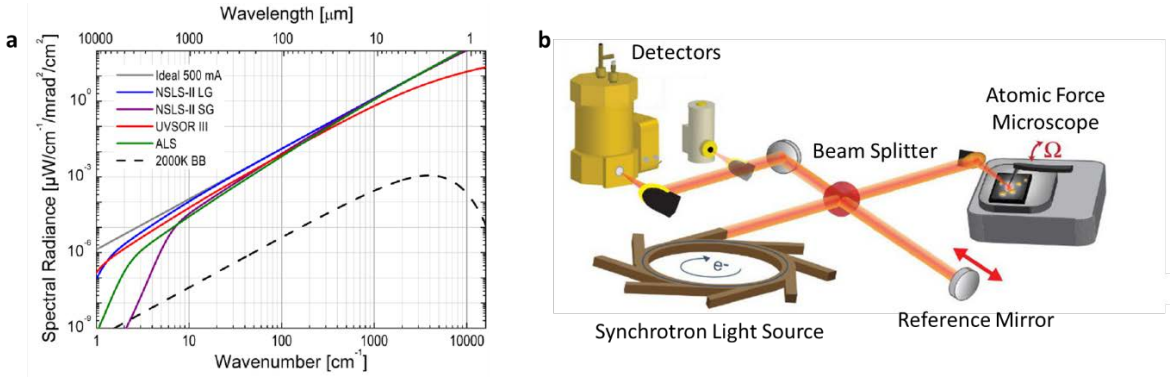

Fig. 1 Synchrotron light sources allow for infrared near-field spectroscopy in an ultrabroadband spectral range. (a) Infrared spectral radiance of different synchrotron light sources in comparison to blackbody (BB) radiation at 2000 K. The large gap (LG) bending magnet at the National Synchrotron Light Source II (NSLS-II) in Upton, USA provides one of the highest infrared spectral radiances of existing synchrotron light sources. Figure adapted from reference [2]. (b) Sketch of a synchrotron infrared near-field spectroscopy (SINS) setup. Figure adapted from reference [3].

In the large part of the infrared spectral region where no suitable table-top laser sources are available, accelerator-based near-field techniques provide an alternative approach [3–6]. As shown in Fig. 1a, synchrotron light sources deliver infrared radiation with several orders of magnitude higher spectral radiance than thermal blackbody radiation [2]. Thus, synchrotron infrared near-field spectroscopy (SINS) enables nanoscale material studies in an ultrabroadband spectral range down to 320 cm^{-1} (9.7 THz) (sketch of a SINS setup shown in Fig. 1b) [3–5].

Referring to Fig. 1a, the National Synchrotron Light Source II (NSLS-II) at Brookhaven National Lab, Upton, USA has a mid- to far-infrared spectral radiance that is among the highest of existing synchrotron light sources [2]. Exploiting this high spectral density, we are currently commissioning a new SINS setup at NSLS-II. At its final stage, we expect our setup to push the spectral limit of SINS to wavenumbers in the range of 100 cm^{-1} [2]. We will illustrate our current SINS capabilities via near-field spectroscopy data of isotropic and anisotropic bulk materials, thin films, and polariton interferometry of 2D and van der Waals materials.

References

[1] Chen, X. et al. 2019. *Adv. Mater.* 31, 1804774.
[2] Dumas, P. & Carr, G.L. *Infrared Spectroscopy and spectro-microscopy with synchrotron radiation.* 2020. Brookhaven National Lab. (BNL), Upton, NY (United States).
[3] Khatib, O. et al. 2018. *ACS Photonics* 5, 2773.
[4] Barcelos, I.D. et al. 2020. *Adv. Opt. Mater.* 8, 1901091.
[5] Yao, Z. et al. 2021. *Nat. Commun.* 12, 2649.
[6] Oliveira, T.V.A.G. et al. 2021. *Adv. Mater.* 33, 2005777.

Near-field hyper-spectral imaging of resonant Mie modes in a dielectric island

Francesca Intonti[1], Nicoletta Granchi[1], Michele Montanari[1], Andrea Ristori[1] Mario Khoury[2], Mohammed Bouabdellaoui[2], Chiara Barri[3], Luca Fagiani[3], Massimo Gurioli[1], Monica Bollani[3], Marco Abbarchi[2]

1. Department of Physics and Astronomy and LENS, University of Florence, Sesto Fiorentino (FI), Italy
2. Aix Marseille Univ, Université de Toulon, CNRS, IM2NP, Marseille, France
3. Istituto di Fotonica e Nanotecnologie (IFN-CNR) and Department of Physics, Politecnico di Milano, 22100 Como, Italy

E-mail: intonti@lens.unifi.it

All-dielectric sub-wavelength sized Mie resonators have emerged in the last decade as promising building blocks for optoelectronic devices, since they provide the possibility to efficiently redirect and concentrate light with low absorption losses [1]. The optical modes in high-index dielectric nanoparticles originate from the excitation of optically induced displacement currents and can be both magnetic and electric in nature. The combination of these two kinds of resonant modes and the exploitation of higher order multipolar modes offers opportunities for directional and polarization controlled emission from nanoemitters [2]. However, the investigation of the intricacies of the Mie resonances at the sub-wavelength scale has been hampered by the limitations of conventional near-field methods. In this work, we address the spatial and spectral mapping of multipolar modes of a Si island by near-field hyper-spectral imaging. A Si resonator, realized by solid state dewetting [3], with diameter of 320 nm and sitting atop a 2 μm SiO_2 substrate, Fig. 1a), is investigated by scanning near-field optical microscopy (SNOM) in scattering configuration, Fig. 1b). The normalized near-field spectrum collected at the apex of the island, illuminated by a tilted supercontinuum laser source, is reported in Fig. 1c), together with the finite difference time domain (FDTD) near-field spectrum. Simulated and experimental spectra are in good agreement, allowing to identify the main higher order multipolar resonances that result from the resonant modes of the antenna. Fig. 1d) shows the near-field map of the resonance at 730 nm, and exploiting the morphology of the sample simultaneously acquired [the island position is highlighted by white circles in Fig. 1d) and e)] allows a direct comparison with the FDTD map of the same resonance, Fig. 1e). Experimental and simulated maps show striking similarities in the spatial distribution of the hot spots that are typical of the mode.

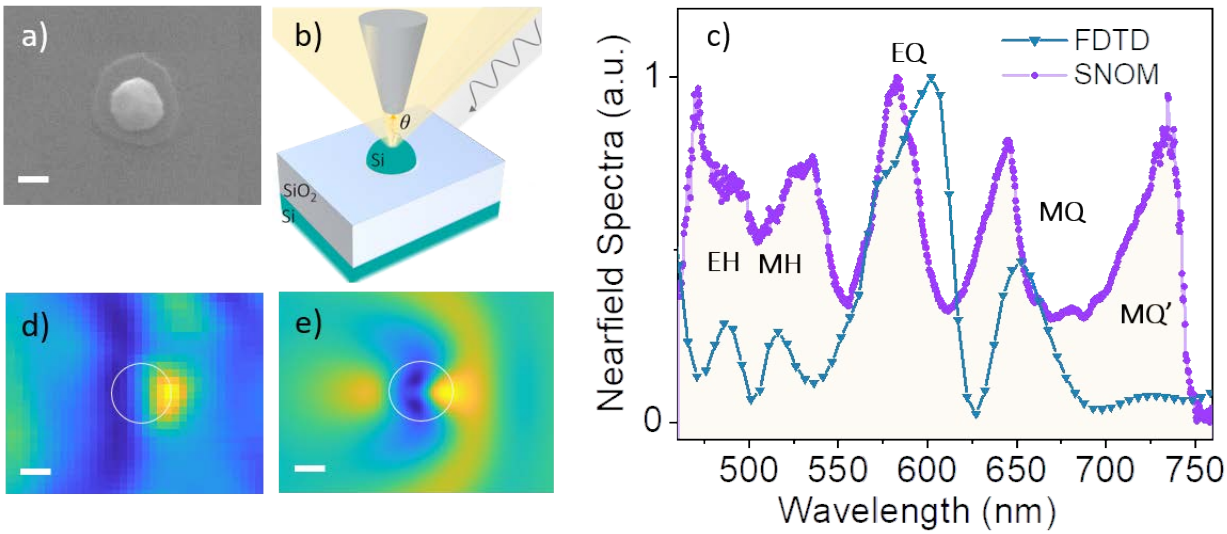

Fig. 1 a) SEM image of a single Si resonator. b) Sketch of the experimental setup: the tilted illumination from the supercontinuum laser is scattered by the island and the scattered light (yellow cone) is collected by an aperture near-field probe. c) Normalized SNOM scattering spectrum collected on top of the dewetted island (purple) and corresponding FDTD spectrum (dark green), the spectral positions of different high order resonances (magnetic and electric quadrupole and hexapoles) are indicated. d) and e) Experimental SNOM and simulated maps relative to the magnetic quadrupole MQ'.

The combination of numerical and experimental results allows a full comprehension of the sensitivity of magnetic light with respect to the thickness of the substrate and the angle of illumination [4]. Moreover, this detailed analysis indicates how such sensitivity affects the near-field scattering pattern of the antenna, suggesting a novel approach to control the position of the localized electric field maxima to engineer an important aspect of the coupling between emitters and antenna: instead of placing the emitter on the hotspot, the hotspot can be moved on the emitter position, offering a versatile tuning tool to control the absorption of the emitter itself.

References

[1] Kuznetsov, A. I. et al., 2016, Science 354, 2472.
[2] Van de Groep , J. et al., 2013, Opt. Express 21, 26285.
[3] Abbarchi, M. et al., 2014, ACS Nano 8, 11181.
[4] Granchi, N. et al., 2021, APL Photonics, 2, 126102.

Observation of the History Dependence of Two Nano-Photoisomerization Pathways in Photochromic Single Crystals

Yuji Arakawa[1], Kazuharu Uchiyama[1], Yuki Hashimoto[2], Kingo Uchida[2], Hirotsugu Suzui[3], Makoto Naruse[3], and Hirokazu Hori[1]

1. University of Yamanashi, 4-3-11 Takeda, Kofu, Yamanashi 400-8511, Japan
2. Ryukoku University, 1-5 Yokotani, Oe-cho, Seta, Otsu, Shiga 520-2194, Japan
3. Department of Information Physics and Computing, Graduate School of Information Science and Technology, The University of Tokyo, 7-3-1 Bunkyo-ku, Tokyo 113-8656, Japan

E-mail: g21tz002@yamanashi.ac.jp

Toward realizing intelligent devices based on the interactions of light and matter, we utilize a photochromic diarylethene single crystal, which is reversibly isomerized into colored and colorless states while maintaining their crystalline state by light irradiation (Fig. 1(a)) [1,2]. Previously, we reported local excitation by local electric field enhancement with an Au-coated metal probe to the surface of a colored photochromic crystal. We found that a chain of photoisomerization was spontaneously formed where nanometer-scale transparent pathways were generated [1]. In other words, a complex pattern was memorized as a result of near-field light excitation. In this study, we examined the *addition* of another memory to existing photon pathways in the photochromic material. We characterized the effects of such additive memory on the original memory or originally formed pathways.

The measurements were performed using a double-probe scanning near-field optical microscope with two probes; one probe was on the upper and the other on the lower side of the crystal sample. After forming a memory path with the upper metal probe, the optical near-field on the rear side was measured within a 2-μm square area by scanning the optical fiber probe (Fig. 1(b)). After forming and observing such a path, which is referred to as "P1" hereafter, we horizontally displaced the local excitation point by an amount of 1 μm and formed another path, of which observation was called "P2". We then returned the local excitation point to the original position and observed the path again (called "P1'") (Fig. 1(c)). Nanoscale near-field optical structures were observed, indicating the formation of two memories. The cross-correlation between P1 and P2 and that between P1' and P2 are demonstrated in Figs. 1(c,i) and 1(c,ii), respectively, for the size of the extracted structure. A negative correlation was observed in the optical near-field scale (~100 nm), indicating that the nanometer-scale memory paths were different from each other regarding different local optical excitation points. The mechanical distortion caused by the first path generation (P1) exclusively constrained the formation of the second path (P2), leading to the formation of different pathways. In other words, a history-dependent effect was observed due to optical near-field excitations added via different positions. Finally, we compared P1 and P1', where local optical excitations were generated at the same point before and after the addition of another memory P2 (Fig. 1(c,iii)). These structures are positively correlated; that is, the structures are consistent for the same local optical excitation even after the addition of path P2. This indicates the conservation of the memory pathways.

These results suggest that the nano-photoisomerization in the photochromic diarylethene single-crystal implements sequential multiple memory structures, where the original memory provides constraints for the subsequent memory formations and is preserved even after the additional path formations. This paves the way for novel functionalities by near-field optics combined with photoisomerization in photochromic materials on the nanometer scale.

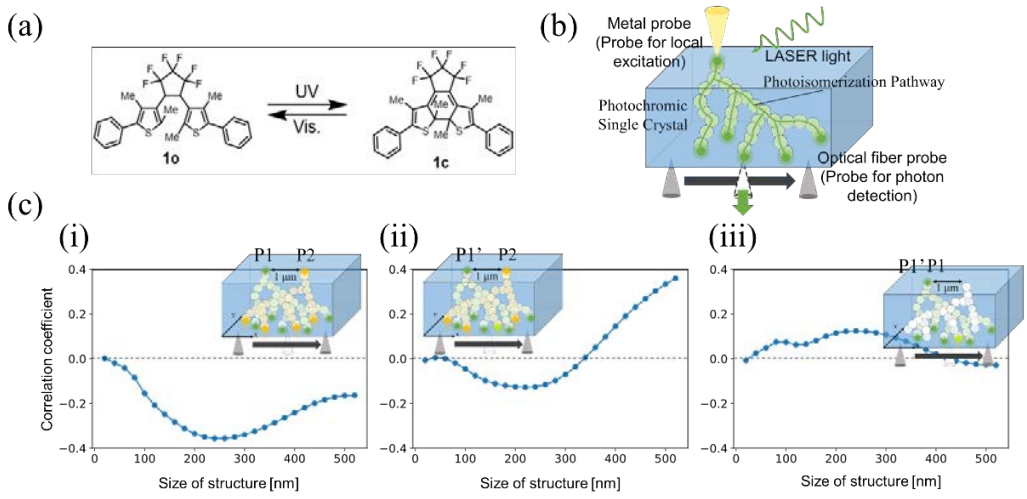

Fig. 1 (a) Photochromic diarylethene molecules and the photoisomerizations. (b) Schematics of the experiments.(c) (i) Cross-correlation of P1 and P2. (ii) Cross-correlation of P1' and P2.(iii) Cross-correlation of P1 and P1' for the size of the extracted structure.

References

[1] Nakagomi, R., Uchiyama, K., Kubota, S., Hatano, E., Uchida, K., Naruse, M., Hori, H., 2018. *App. Phys. A* 124, 10.
[2] Uchiyama, K., Suzui, H., Nakagomi, R., Saigo, H., Uchida, K., Naruse, M., Hori, H., 2020. *Sci. Rep.* 10, 2710.

A Review of Nanoscale Chemical Imaging Applications Using Photo Induced Force Microscopy

Derek B. Nowak[1], **Padraic O'Reilly**[1] **Sung I. Park**[1]

1. Molecular Vista Inc, 6840 Via Del Oro Suite 110, San Jose CA

E-mail: derek@molecularvista.com

Since the original concept of image force microscopy was demonstrated by Kumar Wickramasinghe's group at the University of California, Irvine in 2010 [1], Photo-induced force microscopy (PiFM) as it is now commonly called has seen an incredible expansion into many different scientific disciplines. Applications ranging from biophysics [2], polymer studies [3] and nanoplastics [4], nanocomposites [5], semiconductors [6], geosciences [7], nanoplasmonics [8], and renewables [9]. The ability for PiFM to be sensitive to both organic and inorganic material, operate in a non-contact mode of atomic force microscopy, operate on rough to smooth samples and to be sensitive to monolayers, all while demonstrating the highest spatial resolution nano-IR modality, have all contributed to this success.

The mechanism of PiFM uses mechanical force instead of optical detection to measure the near-field optical interaction between the tip and sample. PiFM leverages local polarization of the sample by tip-enhanced optical illumination, resulting in highly localized forces acting between the tip and sample which are easily detected by AFM. Mechanical detection eliminates the problem of background scattering seen in s-SNOM, giving PiFM a superior SNR and greatly enhancing ease-of-use and quality of data on most samples. The basic tip-sample optical interaction in s-SNOM and PiFM is quite similar – the same near field illumination and local polarization of the sample that emits scattered photons in s-SNOM also generates the mechanical forces detected in PiFM [1]. Thus, one might expect s-SNOM and PiFM to have similar spatial resolution; however, PiFM generally shows superior resolution by virtue of its increased SNR for a given tip radius. In PiFM, the tip-sample interface generates two types of short-range forces: (1) the usual van der Waals (vdW) force that NC-AFM relies on for mapping the topography of the sample surface, and (2) the photo-induced force (PiF) generated by near field illumination. Both forces act over a very short range, coming into play only when the tip is atomically close to the sample surface (~10 nm or less). PiFM utilizes two vibrational modes of the rectangular AFM cantilever to measure the two forces independently – the interatomic vdW force with one mode, and the photo-induced force (PiF) with another. Since the vibration of the two modes is completely independent, motion in one mode generally does not influence the other. Assigning each of these forces to its own vibrational mode of the cantilever is accomplished by modulating the vdW force at or near the resonant frequency of one mode (as is normally done in NC-AFM by mechanically driving the cantilever vibration and monitoring its response) and modulating or pulsing the excitation light so that it generates the PiF at the resonant frequency of another cantilever mode. Due to the high quality-factor Q of the cantilever resonance, even tiny forces in the range of pN can excite measurable oscillations, making this approach ideal for measuring small photo-induced forces.

A review of published PiFM work on nanoscale applications will be presented, showcasing this new-frontier technique and it's potential. Many recent developments in real world applications, in process monitoring and defect review on unpublished applications and use cases will be presented.

References

[1] Rajapaksa, I.; Uenal K.; Wickramasinghe H. K., Appl. Phys. Lett. **2010**, 97, 073121.
[2] Eesaee, M.; et.al. *ACS Appl, Polym. Mater.* **2022**, 4, 4, 301-312.
[3] Sunday, D. F.; et. al. *Chem. Mater.* **2020**, 32, 6.
[4] I. C. ten Have; et. al. *Chemistry – Methods* **2021**, 1(5), 205–209.
[5] Eichmann, S.; Nowak, D.; Jacobi, D., Burnham, N. *Microsc Microanal,* **2018**, 24, S1, 1040-1041.
[6] Huang, Y.; et. al. *ACS Photonics* **2018**, 5, 11, 4352-4359.
[7] Otter, L.M.; Förster, M.W.; et.al. *GGR Cutting-Edge Review: Geostand Geoanal Res*. **2021**, 45, 5–27.
[8] Tumkur, T. U.; Yang, X.; Cerjan, B.; Halas, N. J.; Nordlander, P.; Thomann, I. *Nano Lett.* **2016,** *16* (12), 7942-7949.
[9] Song, J.; et. al. *Adv Sci Comm* **2020**, 7, 2001986

Structural and Optical Identification of Planar Side-Chain Stacking P3HT Nanowires

He-Chun Chou[1], Chung-Kai Fang[2], Pei-Yun Chung[3], Jia-Ru Yu[1], Ing-Shouh Hwang[2], Jiun-Tai Chen[3], and Chi Chen[1,*]

1. Research Center for Applied Sciences, Academia Sinica, Taipei, Taiwan
2. Institute of Physics, Academia Sinica, Taipei, Taiwan
3. Department of Applied Chemistry, National Yang Ming Chiao Tung University, Hsinchu, Taiwan
E-mail: chenchi@gate.sinica.edu.tw

Poly(3-hexylthiophene) (P3HT) is well-recognized for forming π–π stacked crystalline films and nanowires. In this study, we identified a new planar crystalline P3HT architecture assembled by hexyl side chains by building a home-made scanning near-field optical microscopy and confocal microscopy in glove box.[1] The atomic force microscopy results indicated that both the π–π stacking and side-chain stacking nanowires were crystalline ribbons decorated with amorphous fringes. The different stacking structures of the nanowires led to different interchain coupling strengths and hence spectroscopic properties. Both types of nanowires were characterized using confocal microscopy and home-made scanning near-field optical microscopy. The coexistence of the planar side-chain stacking structure in P3HT films and nanowires along with the π–π stacking architecture leads to multiplicity in their optical properties.[2]

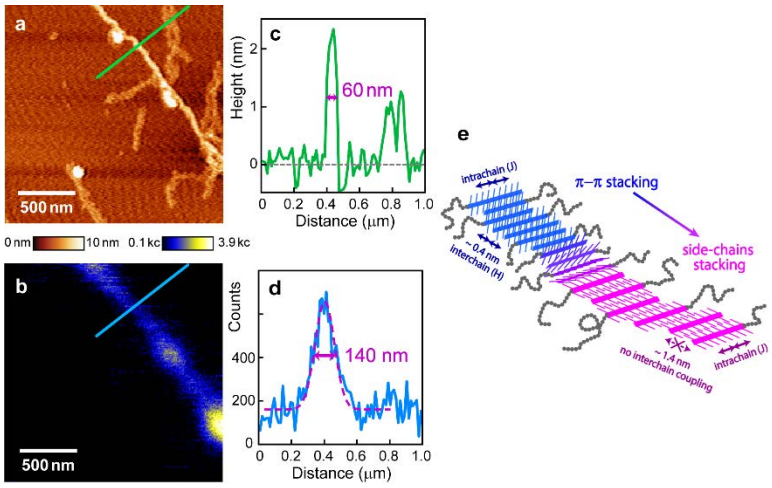

Fig. 1 SNOM-fluorescence imaging of the P3HT NWs. (a and b) Simultaneously recorded AFM topography (a) and SNOM-fluorescence intensity map (b) of the P3HT NWs. Cross-sectional profiles of the linecuts in (a) and (b), respectively. (e) Structural model of the transition from the π–π stacking to the side-chain stacking in the NWs. The directions of interchain and intrachain coupling were also indicated.

.

References

[1] Yu, J.-R.; Chou, H.-C.; Yang, C.-W.; Liao, W.-S.; Hwang, I.-S.; Chen, C. 2020, *Rev. Sci. Instrum.* 91, No. 073703.
[2] Chou, H.-C.; Fang, C.-K.; Chung, P.-Y.; Yu, J.-R.; Liao, W.-S.; Chen, S.-H.; Chen, P.; Hwang, I.-S.; Chen, J.-T. and Chen, C. 2021, *Macromolecules* 54, 10750−10757

Using Dispersive Lossy Media to Narrow Plasmon Linewidths

Ryan Peck[1], **Ali Khademi**[1], **Juanjuan Ren**[2], **Stephen Hughes**[2], **Alex Brolo**[1], **Reuven Gordon**[1]

1. University of Victoria, 3800 Finnerty Rd., Victoria, BC, Canada, V8W 2Y2

2. Queen's University, 99 University Ave., Kingston, ON, K7L 3N6

E-mail: rpeck34@gmail.com

It is known that the presence of loss in plasmonic systems broadens plasmon linewidths. This relationship is explicitly displayed in the commonly used formula for the linewidth of a plasmon in spectral units: $\Gamma[\text{eV}] = \frac{\hbar}{T_2}$, where T_2 is the total decay time of the plasmon [1]. The linewidth of a plasmon peak in nm is given by $\Gamma[nm] = \frac{\lambda_0 \Gamma[\text{eV}]}{E_0}$ where λ_0 is the plasmon resonance wavelength and E_0 is the plasmon resonance energy in eV. Adding loss to the surrounding medium then allows for plasmons to exchange their energy with the absorbing medium, so that T_2 is necessarily decreased which results in an increase in the plasmon linewidth.

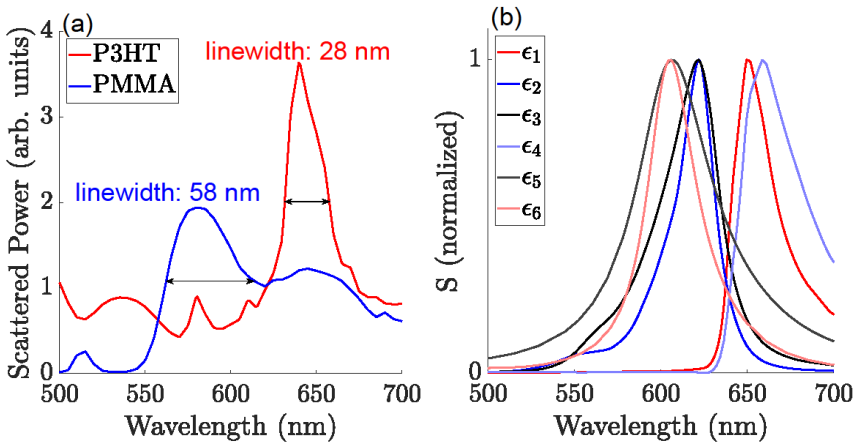

Fig. 1 (a) Scattered power for 20 nm gold encased in PMMA and P3HT obtained using a dark field microscope. The linewidths are the full width at half the maximum (FWHM) of each of the peaks. (b) COMSOL simulations for a 20 nm gold nanoparticle embedded in 120 nm layers of various surrounding media. The media used in (b) were: $\varepsilon_1 = \varepsilon_{\text{P3HT}}$, $\varepsilon_2 = \text{Re}\{\varepsilon_{\text{P3HT}}\}$, $\varepsilon_3 = \text{Re}\{\varepsilon_{\text{P3HT}}\} + 0.3i$, $\varepsilon_4 = 5 + \text{Im}\{\varepsilon_{\text{P3HT}}\}i$, $\varepsilon_5 = 5 + 0.3i$ and , $\varepsilon_6 = 5$.

Dark field microscopy was used to measure the scattering signal from 20 nm gold nanoparticles encased in 120 nm thin layers of both lossy and non-lossy materials to determine the plasmon linewidths. The organic polymer P3HT, commonly used in organic photovoltaics, was used as the lossy medium and PMMA was the non-lossy medium. The results of the dark field measurements are shown in Fig. 1 (a). Intuitively, and as expected from the linewidth formula shown above, adding loss to the surrounding medium should broaden plasmon linewidths [2], but here we see the opposite; P3HT has a much narrower cross section than PMMA. To verify this odd result, Lumerical FDTD simulations were performed which showed good agreement with the measured spectra.

Using a Green function scattering theory, it was found that the dispersion in both the real and imaginary parts of the permittivity have a significant impact on the plasmon linewidth. Figure 1 (b) shows the results of COMSOL simulations, which calculated the Green function propagator, S, for a 20 nm gold nanoparticle embedded in a variety of 120 nm thick surrounding media. PMMA is not dispersive while P3HT has a large dispersion for both the real and imaginary parts of the permittivity near the plasmon peak. In the Rayleigh scattering regime, the plasmon resonance condition for a small nanoparticle is met when $\varepsilon_1 = -2\varepsilon_2$, where ε_1 is the nanoparticle permittivity and ε_2 is the permittivity of the surrounding medium. The plasmon resonance is swept through much faster for P3HT than for PMMA due to the high dispersion of P3HT which causes a reduction in the plasmon linewidth. Also, the magnitude of the permittivity plays an important role in narrowing linewidths. In Fig. 2, the $\varepsilon_6 = 5$ peak has a narrow linewidth of 28 nm, even without dispersion. This is because, although the surrounding medium lacked dispersion, a large real permittivity red shifts the plasmon peak into a region where gold has a high dispersion, and so this greater dispersion in the gold nanoparticle narrows the linewidth. Therefore, the commonly used linewidth formula is inaccurate when considering dispersive and lossy media such as P3HT, and when dispersion is involved, lossy media can even yield narrower linewidths than non-lossy media.

References

[1] Maier, S.A. Localized Surface Plasmons, *"Plasmonics: Fundamentals and Applications"*. 2007, Springer Science+Business Media LLC, 233 Spring Street, New York, NY, page 75.

[2] Mishchenko, M. I., and Janna M. D. 2019, "Plasmon resonances of metal nanoparticles in an absorbing medium", OSA Continuum 2.12, 3415-3421.

Coherent control of plasmon interferences in 2D crystalline cavities for Boolean calculation

Florian Dell'Ova[1], **Diana Shakirova**[1,3], **Yoann Brulé**[1], **Laureen Moreaud**[2], **Gérard Colas-Des-Francs**[1], **Erik Dujardin**[1,2] **and Alexandre Bouhelier**[1]

1. Laboratoire Interdisciplinaire Carnot de Bourgogne, CNRS UMR 6303, Université Bourgogne Franche-Comté, Av. A. Savary, 21000 Dijon, France
2. CEMES, CNRS UPR 8011, 29 rue J. Marvig, 31055 Toulouse, France
3. Faculty of Physics of ITMO University, Ronverksky Pr. 49, bldg. A, St. Petersburg, 197101, Russia.
E-mail: florian.dell-ova@u-bourgogne.fr

We are exploring a strategy for optical information processing by developing an integrated planar plasmonic calculator [1]. The device we propose is a 2D modal plasmonic cavity made of crystalline gold, as shown in Fig.1A. The double hexagonal shape of the cavity is engineered by Focus Ion Beam milling. This specific shape offers a rich plasmon modal landscape enabling the transport and the treatment of the optical information through the device. The input and output nodes, defined by the apexes of the double hexagon, are linked via interacting plasmon modes. Surface plasmons convert the near-infrared incoming laser femtosecond pulses into visible photons in order to build the desired logical operations in remote region of the device[2,3]. This wavelength up-conversion, called nonlinear photoluminescence (nPL), is a sensitive nonlinear probe for the plasmon local electric field [4] and characterizes the outputs of the logic gate (see fig.1 B).

Controlling the interaction between mobilized surface plasmons is a critical point in the operation of the calculator. This is achieved by adjusting the polarization of the entry nodes and controlling the phase of the plasmon interference pattern. To do so, we implemented a spatially steerable diffraction-limited temporally-synchronized dual excitation nodes capable of accommodating any non-trivial device geometry. Our control strategy allows for an agile reconfiguration of truth table of the logic gate. The Boolean values are encoded on the input nodes into the polarization states of the two optical stimuli feeding the calculator.

With this specific geometry, we are able to reconstruct the truth table of all basic logic operations [5]. Taking advantage of the coherent effects when the input nodes are temporally synchronized, we demonstrate an XOR gate and a half-adder based on plasmon interferences.

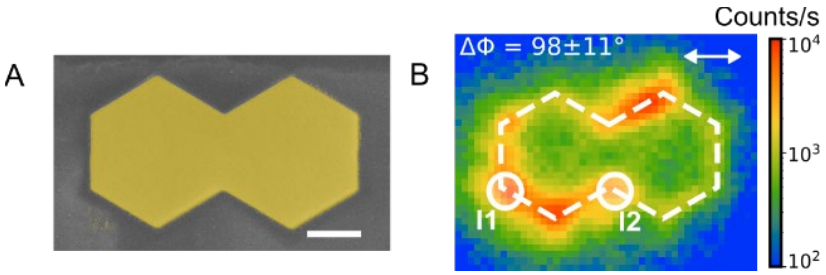

Fig. 1 A. Colorized scanning electron microscopy image of a double hexagonal shaped Au cavity. The white scale bar is 500 nm. B. Nonlinear photoluminescence wide field image of the cavity under two beams excitation, positioned in I1 and I2 respectively. Both beams are horizontally polarization (white arrow) and the relative phase between the two pulses is 98 ± 11°.

References

[1] Kumar, U. et al. 2018. *ACS Photonics*, vol. 5, no. 6, pp. 2328–2335.
[2] Viarbitskaya, S., Demichel, O., Cluzel, B., Colas des Francs, G., and Bouhelier, A. 2015. *Phys. Rev. Lett.*, vol. 115, no. 19, p. 197401.
[3] Agreda, A. et al. 2019. *ACS Photonics*, vol. 6, no. 5, pp. 1240–1247.
[4] Bouhelier, A., Bachelot, R., Lerondel, G., Kostcheev, S., Royer, P. and Wiederrecht, G.P. 2005. *Phys. Rev. Lett.*, vol. 95, no. 26, p. 267405.
[5] Kumar, U. *et al. 2021. ACS Nano*, vol. 15, no. 8, pp. 13351–13359.

Analytic methods to study the properties of electromagnetic waves in plasmonic slot waveguides

Amrita Pati[1] **& Reuven Gordon**[1]

1. Department of Electrical and Computer Engineering, University of Victoria, 3800 Finnerty Road, Victoria, British Columbia, V8P 5C2, Canada

rgordon@uvic.ca

Plasmonic slot waveguides produce highly localized electromagnetic (EM) fields over a wide range of frequencies which makes them suitable for applications varying from modulators [1] to optical tweezers [2]. They support modes with long propagation lengths and high group velocities in the optical communication regime [3], allow sharp bending angles at lower levels of losses [4], and are easy to fabricate. In addition, the metal layers provide contacts down to the subwavelength scale and being good thermal conductors, improve heat dissipation in the circuitry [5]. Among several other applications, these properties of gap plasmon-based waveguides can be used to interface Si photonics and electronics which can potentially lead to highly miniaturized and faster communication devices.

However, their practical implementation requires reliable computation of several waveguide parameters and determination of metal geometry that optimizes the performance of the structure. Several works in the past have analyzed the metal-insulator-metal structures but the majority of them use the numerical analysis approach. Numerical simulations are resource-intensive and do not offer any insights into the actual interactions taking place between the EM waves and the metal. Our goal here is to build a simple theoretical framework to explain the reflection and propagation of EM waves in the slot, compute their modal properties, and identify the desired optimal configuration.

In our previous work, we studied the 2-D slit geometry in real metals [6]. We derived an analytic expression for reflection coefficient in the slit using the effective index approximation. Our approach eliminated the need for any numerical techniques including numerical integration. We compared the values of the reflection phase with a past work and found agreement to within 0.06 rad [7]. The Fabry-Pérot model was used to calculate the optical cross-sections, field intensity, and power inside the slit and this allowed us to establish the condition for maximum power transfer in the slit as shown in Fig. 1(a). The narrowest slits generated the highest field intensities but in contrast, the power peaked for slit configurations that produced equal scattering and absorption cross-sections at resonance.

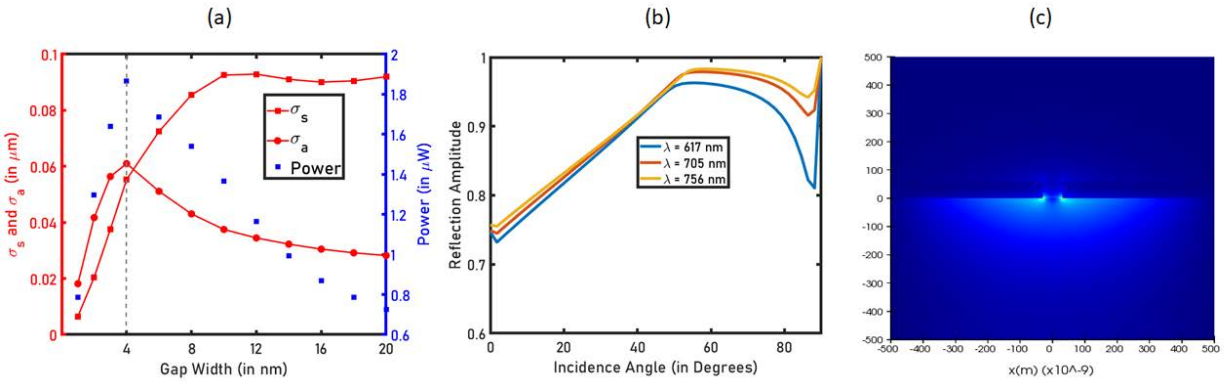

Fig. 1 (a) Variation of power, optical cross-sections with the width of a slit, power in the slit is maximum for equal values of scattering (σ_s) and absorption (σ_a) cross-sections at resonance. (b) Reflection amplitude vs incidence angle in a plasmonic slot waveguide of width 30 nm at different wavelengths (617 nm, 705 nm, 756 nm). (c) Lumerical FDTD simulations showing the electric field in a 60 nm slot waveguide on a glass substrate

In our current work, we focussed on a 3-D plasmonic slot waveguide. Linearly polarized EM waves were incident on the slot at an angle θ**.** First, we derived an analytic equation for the reflection coefficient in the slot by assuming the metal to be a perfect conductor. Next, we invoked the effective index approximation to incorporate the losses of a real metal into our equation. Fig. 1(b) shows the theoretically calculated values of reflection amplitude in the slot waveguides for different wavelengths. They were validated against numerical FDTD simulations. The values of the reflection coefficient were used to determine the guiding condition for the waveguide and other modal properties such as group velocity and propagation length which are key in designing high-performance plasmonic slot waveguides.

References

[1] Haffner, C., Heni, W., Fedoryshyn, Y., Niegemann, J., Melikyan, A., Elder, D. L., Salamin, Y., Josten, A., Koch, U., Hoessbacher, C., Ducry, F., Juchli, L., Emboras, A., Hillerkuss, D., Kohl, M., Dalton, L. R., Hafner, C., Leuthold, J., 2015. *Nat. Photon*., 9, 525-528

[2] Pang, Y., Gordon, R., 2012. *Nano Lett.*, 12, 402-406

[3] Veronis, G., Fan, S., 2005. *Opt. Lett.*, 30, 3359-3361

[4] Liu, L., Han, Z., He, S., 2005. *Opt. Express*, 13, 6645-6650

[5] Gordon, R., Dobinson, M., 2021. *Opt. Mater. Express,* 11, 2192-2196

[6] Pati, A., Gordon, R., 2021. *Opt. Express*, 29, 38129-38139

[7] Sharifi, Z., Gordon, R., 2022. *Plasmonics* 17**,** 315–320

Plasmonic nonlinear response from hBN nanoflakes excited with a CW laser

Mirali Seyed Shariatdoust[1], **Michael Dobinson**[1], **Ghazal hajisalem**[1], **Reuven Gordon**[1]

1. Department of Electrical and Computer Engineering, University of Victoria, Victoria, British Columbia V8P 5C2, Canada

E-mail: mseyedshariatdoust@uvic.ca

Trapping single hexagonal boron nitride (hBN) nanoflakes in a double nanohole using optical tweezers made it possible to obtain a nonlinear response from sub-diffraction limit area where it was pumped with low power continuous wave laser (~10 mW). Here, we demonstrate second harmonic generation (SHG) at 486.5 nm from the hBN nanoflakes mixed with gold nanorods illuminated at 973 nm. It is promising to use the gold nanorods with resonance tuned at 973 nm since they provide around 1000 times more electric field intensity over double nanoholes. The SHG is not resolved from the nanorods alone, or the nanoflakes in absence of the nanorods. This scheme can be used in telecommunications band signal detection using silicon-based detectors and ultra-fast imaging [1,2].

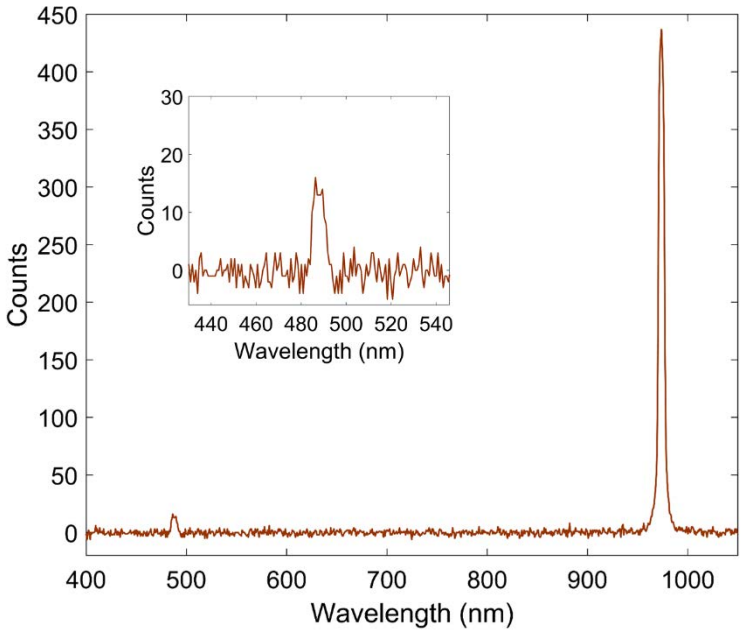

Fig. 1 Initial source (973 nm) and second harmonic signal (486.5 nm) spectrum

References

[1] Hajisalem, G., Shariatdoust, M. S., Ali, R. F., Gates, B. D., Barclay, P. E., and Gordon, R. 2021. *ACS Photonics,* Single nanoflake hexagonal boron nitride harmonic generation with ultralow pump power, 8(7), 1922-1926.

[2] Yao, K., Yanev, E., Chuang, H. J., Rosenberger, M. R., Xu, X., Darlington, T., McCreary, K. M., Hanbicki, A.T., Watanbe, K., Taniguchi, T., Jonker, B.T., Zhu, X., Basov, D.N., Hone, J.C., and Schuck, P. J. 2019. . *ACS Nano,* Continuous wave sum frequency generation and imaging of monolayer and heterobilayer two-dimensional semiconductors, 14(1), 708-714.

Fundamental limits and complete coupling of light into polaritons

Eduardo J. C. Dias[1], **F. Javier García de Abajo**[1,2]

1. *ICFO - Institut de Ciencies Fotoniques, The Barcelona Institute of Science and Technology, 08860 Castelldefels (Barcelona), Spain*
2. *ICREA - Institució Catalana de Recerca i Estudis Avançats, Passeig Lluís Companys 23, 08010 Barcelona, Spain*

E-mail: eduardo.dias@icfo.eu

Polaritons in metals and 2D materials have been extensively studied over the past decade due to their fundamental interest and as a platform for applications in telecommunications and sensing. The wavelength of these polaritons is generally small compared to that of a photon of the same frequency, making them very attractive to manipulate light at deep-subwavelength distances. However, it simultaneously introduces a challenge in the coupling between propagation light and plasmonic modes, since the momentum mismatch between the two makes the in/out-coupling of this process intrinsically weak.

In this work, we address some fundamental limits in the coupling of radiation to surface polaritons [1]. We study the scattering properties of point-like scatterers over a polariton-supporting surface and quantify the coupling of light-to-polaritons cross-section for this process as a function of the scatterer effective polarizability. We further find a generalization of the optical theorem to surface polaritons, which remarkably leads to a fundamentally maximum limit on light-to-polariton coupling cross-section, under plane-wave illumination.

We furthermore show that the fundamental limit described above can be overcome by a small scatterer placed at a suitable distance from a planar surface, under illumination by an adequately focused light beam [2]. We present rigorous closed-form prescriptions for the modulation of the incident light beam which maximizes this coupling, depending on the characteristics of the scatterer and surface, and show that it can lead to complete coupling to surface polaritons (Fig. 1a). We corroborate the analytical results by performing rigorous fully-numerical simulations using realistic setups, which exhibit a very strong enhancement of the absorption into surface plasmons under the prescribed optimal conditions (Fig. 1b,c).

Our results open a practical route to circumvent the long-standing photon-polariton wavelength mismatch problem in Nanophotonics.

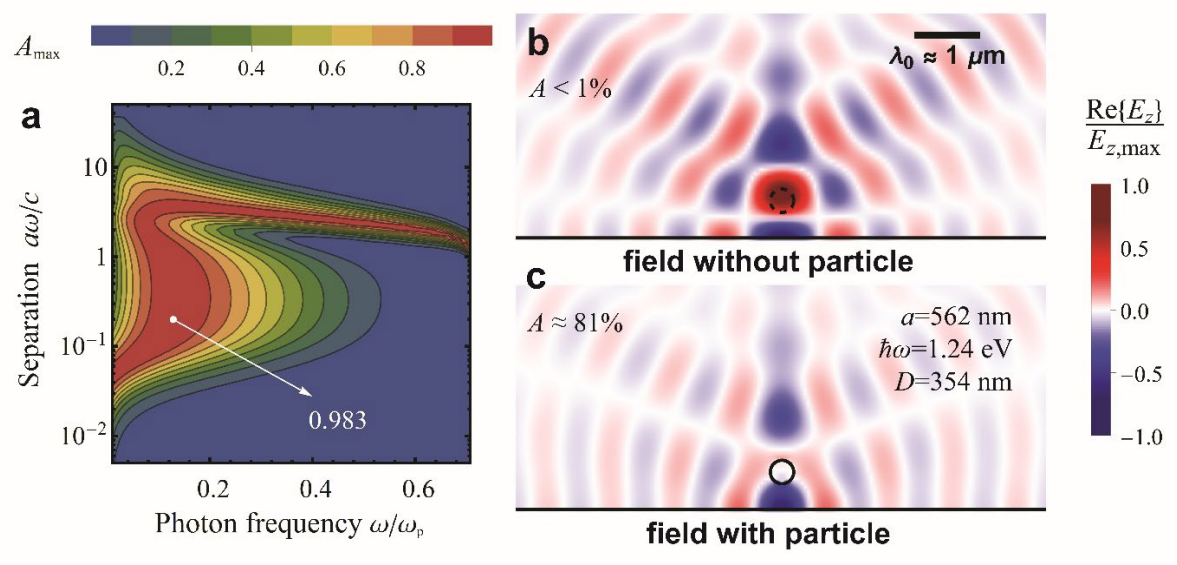

Fig. 1 (a) Dependence of the maximum coupling fraction A_{max} on frequency ω and particle-surface separation a for a point dipole above a semi-infinite Drude metal film with plasma frequency ω_p and damping $\omega_p/100$, approaching 100% for a wide combination of the two parameters. (b,c) Numerical simulations of the near-field under optimal illumination in the (a) absence and (b) presence of a Si spherical scatterer with diameter D (represented by open and solid circles, respectively) at a distance a from the surface of a Ag semi-infinite-film. The presence of the Si sphere enhances the absorption into silver plasmons to ~80%.

References

[1] E.J.C.Dias and F.J. García de Abajo, "Fundamental Limits to the Coupling between Light and 2D Polaritons by Small Scatterers." ACS Nano **13**, 5184 (2019).

[2] E.J.C.Dias and F.J. García de Abajo, "Complete Coupling of Focused Light to Surface Polaritons." Optica **8**, 520 (2021).

Engineering circular dichroism of stretchable chiral metamaterial

Florian Lamaze[1], Jérémie Béal[1], Julien Proust[1], Louis Giraudet[2]

1 Light, nanomaterials, nanotechnologies EMR 7004, Université de Technologie de Troyes, 10004 Troyes
2. Laboratoire De Recherche en Nanosciences (LRN) - EA 4682, Université de Reims Champagne-Ardenne, 51687 Reims
E-mail: florian.lamaze@utt.fr

Due to their confined and enhanced localized electric field, plasmonic nanostructures are systems providing extreme sensitivity to their close environment. Consequently, the deformation of a flexible substrate permits the modulation of the Localized Surface Plasmon Resonance (LSPR) of plasmonic gold nanostructures via the induced change in the geometry [1]. This should allow the development of high sensitivity deformation sensors.

The 2D chirality of gold nanoparticles on a substrate leads to a large change in the LSPR depending on the direction of rotation of a circularly polarized source. This introduces the notion of circular dichroism (CD) which corresponds to the difference in response between right and left polarization. Since chirality is strongly dependent on geometry, it can be expected that a change in the latter *via* the application of a deformation leads to a significant variation in circular dichroism [2].

The chosen chiral antenna is composed by a central cylinder with six "satellites" ellipsoids, as shown on Fig.1 (a). We used electron beam lithography to fabricate the structure on solid substrate, as shown on the SEM image on Fig.1 (b), and then transferred on a flexible substrate with a homemade process.

Here, we present the results of a combined numerical and experimental study. We used the Finite Difference Time Domain (FDTD) method to optimize the circular dichroism and its variation, as shown on Fig.1 (c,d), via the implementation of a homemade deformation model. The circular dichroism variation was experimentally investigated and compared with numerical simulations thanks to *in situ* scattering measurement with an integrating sphere.

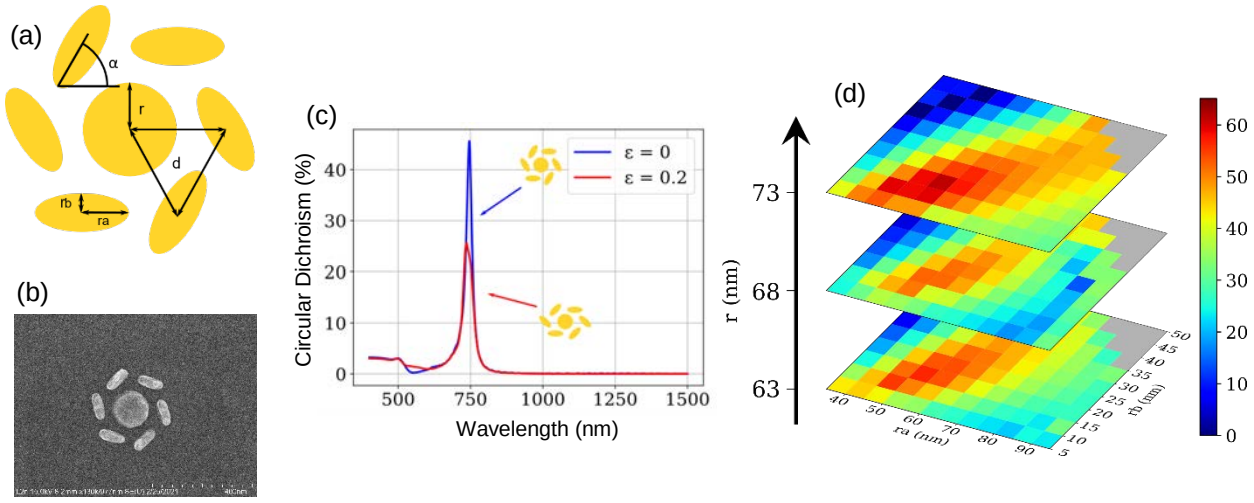

Fig. 1 (a) Schematic of the structure consisting of a central cylinder with six "satellites" ellipsoids and the associated parameters. (b) SEM image of the structure. (c) FDTD Circular Dichroism spectra of the structure at 0% and 20% of deformation. (d) FDTD maps of the maximum CD as a function of different parameters.

References

[1] Cataldi, U. Caputo, R. Kurylyak, Y. Klein, G. Chekini,C.U. Bürgi, T. 2014. *J. Mater. Chem. C*, 2(37), 7927-7933
[2] Zu, S. Bao, Y. Fang, Z. 2016. *Nanoscale,* 8(7), 3900-3905

Exciting and mapping directional surface plasmon polaritons using automated dual-tip scanning near-field optical microscope

Najmeh Abbasirad [1], Angela Barreda[2], Michael Steinert[1] , Yi-Ju Chen[3] , Isabelle Staude [2], Jer-Shing Huang[3], Frank Setzpfandt[1, 4] and Thomas Pertsch [1, 4]

1. Institute of Applied Physics Abbe Center of Photonics Friedrich-Schiller-Universität Jena, Albert-Einstein-Str. 15, 07745 Jena, Germany
2. Institute for Solid State Physics, Friedrich Schiller University, Helmholtzweg 3, 07743 Jena, Germany
3. Research Department of Nanooptics, Leibniz Institute of Photonic Technology, Albert-Einstein Str. 9, 07745 Jena, Germany
4. Fraunhofer Institute of Applied Optics and Precision Engineering, Albert-Einstein-Str. 7, 07745 Jena, Germany

E-mail: najmeh.abbasirad@uni-jena.de

Using the dual-tip scanning near-field optical microscope (SNOM), we experimentally measured directional surface plasmon polaritons (SPPs) at an air-gold interface excited by a dipolar emission from an aperture tip. The experimental results are supported by numerical simulations based on the Bethe-Bouwkamp model.

Different geometries, including slits and nanoantennas, have been shown to excite SPPs with directional properties[1-2]. In this work, an automated dual-tip SNOM was used to map directional SPPs in the near-field of an air-gold interface [3]. Two aperture tips of an automated dual-tip SNOM were exploited to excite and map the SPP pattern in the near-field. To perform the near-field measurement, the excitation tip was stationary, illuminating a monocrystalline gold platelet at a wavelength $\lambda_0 = 1.55\ \mu m$, and the excitation tip mapped the SPPs near-field angular pattern around the excitation tip.

Figures 1(a) and (b) show SEM images of the excitation and detection tip apex, respectively. The directional measured near-field pattern of the SPPs is observed in Fig. 1(c). When the excitation aperture tip is considered as a nanoantenna, due to its geometry, the directional pattern results from both in-plane magnetic and out-of-plane electric dipoles excitation [4-5].

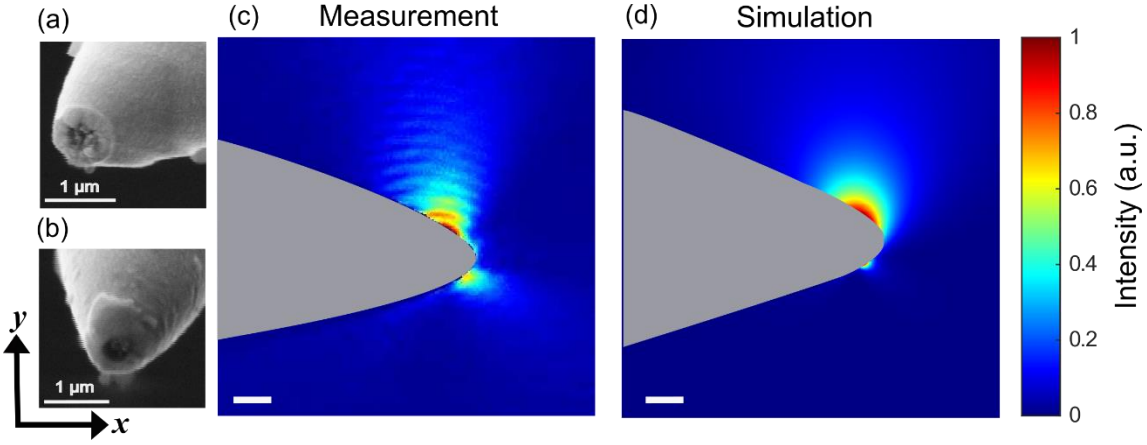

Fig. 1 SEM images of (a) excitation (b) detection tips. (c) Near-field measurements of the SPPs directional propagation due to the dipolar emission from the excitation aperture tip. (d) Simulated magnetic field intensity. The scale bar denotes 1 µm.

To simulate the SPPs angular distribution pattern, we have used the Bethe-Boukamp model employing an out-of-plane electric dipole and in-plane magnetic dipole at the center of the aperture. Figure. 1(d) depicts the corresponding magnetic field intensity calculated in a plane 20 nm above the gold platelet, using the FDTD Solver Lumerical. In parabolic-like gray regions, no optical data is accessible. The good agreement between the measured near-field and the simulation verifies that the out-of-plane electric and in-plane magnetic dipoles are excited due to the asymmetry of the aperture tip apex geometry.

References

[1] Rodríguez-Fortuño, F. J., Marino, G., Ginzburg, P., O'Connor, D., Martínez, A., Wurtz, G. A., & Zayats, A. V. (2013). Near-field interference for the unidirectional excitation of electromagnetic guided modes. Science, 340(6130), 328-330.

[2] Xi, Z., Lu, Y., Yu, W., Wang, P., & Ming, H. (2014). Unidirectional surface plasmon launcher: rotating dipole mimicked by optical antennas. Journal of Optics, 16(10), 105002.

[3] Abbasirad, N., Berzins, J., Kollin, K., Saravi, S., Janunts, N., Setzpfandt, F., & Pertsch, T. (2019). A fully automated dual-tip scanning near-field optical microscope for localized optical excitation and detection in the visible and near-infrared. Review of Scientific Instruments, 90(5), 053705.

[4] Rotenberg, N., Krijger, T. L., Le Feber, B., Spasenović, M., de Abajo, F. J. G., & Kuipers, L. (2013). Magnetic and electric response of single subwavelength holes. Physical Review B, 88(24), 241408.

[5] Novotny, L., & Hecht, B. (2012). Principles of nano-optics. Cambridge university press.

Towards complete optical coupling to ultraconfined surface polaritons

Saad Abdullah[1], Jan Krpensky[1], Eduardo J. C. Dias[1], Vahagn Mkhitaryan[1,2], F. Javier García de Abajo[1,3]

[1]*ICFO - Institut de Ciencies Fotoniques, The Barcelona Institute of Science and Technology, 08860 Castelldefels (Barcelona), Spain*

[2] *School of Electrical and Computer Engineering, Birck Nanotechnology Center and Purdue Quantum Science and Engineering Institute, Purdue University, West Lafayette, IN 47906, USA*

[3]*ICREA-Institució Catalana de Recerca i Estudis Avançats, Passeig Lluís Companys 23, 08010 Barcelona, Spain*

Abstract: We experimentally demonstrate high coupling of light to surface polaritons by means of an optimized scatterer placed at a suitable distance from a polariton-supporting surface. Specifically, we consider poorly-absorbing gold disks acting as nearly-perfect resonant scatterers, which we separate from a gold film by means of a dielectric silica spacer. This configuration leads to resonant coupling between externally incident light and plasmon polaritons in the film with associated cross sections that approach the fundamental limit $\sim\lambda^2$ imposed by the light wavelength λ. Our method introduces a disruptive, efficient way to solve the in/out-coupling problem in nanophotonics.

We experimentally demonstrate a high coupling of light to surface polaritons by means of optimized scatterers placed at a suitable distance from a polariton-supporting surface. Specifically, we consider poorly-absorbing gold disks acting as nearly-perfect resonant scatterers, which we separate from a gold film by means of a dielectric silica spacer. In this configuration, the scatterer develops a strong induced dipole under external illumination tuned to the particle resonance, which mediates the coupling between light and surface polaritons. However, if the scatterer is too close to the surface, the resonance is quenched by the very same coupling that we intend to achieve, thus reducing the overall dipolar strength and, consequently, the efficiency of the coupling scheme. By separating the particle from the surface, an optimum distance is found for which a compromise between resonance strength (increasing with separation) and efficiency of coupling (decreasing with separation) is optimized. Here, we report experimental results showing nearly complete coupling by means of gold-disk scatterers coupled to plasmon polaritons in a planar gold surface. To this end, we measure the infrared reflectance spectra of the scatterer-spacer-surface system, from which we extract the effective polarizability as well as the associated coupling cross sections, which approach the fundamental limit $\sim\lambda^2$ imposed by the light wavelength λ. Our experimental data are in agreement with numerical simulations, which we complement with analytical theory. These findings provide a disruptive, efficient approach to solving the long-standing problem of unity-order in/out coupling in nanophotonics.

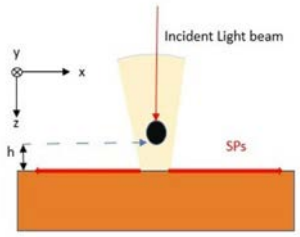

Fig 1: Scheme of the coupling configuration and working principle. A dipolar scatterer is placed close to a polariton-supporting substrate and illuminated under normal incidence conditions. The scatterer develops an induced dipole that couples to the surface polaritons. If the scatterer is placed too close to the surface, the light emission that it produces (i.e., the scattered field) is strongly quenched by the sought-after coupling to polaritons, thus reducing the overall dipolar strength of the combined scattered-substrate system. By separating the particle from the surface, an optimum distance is found for which the compromise between large strength (increasing with separation) and strong coupling to polaritons (increasing with decreasing distance) is optimized.

References

[1] Z. Liang, L. Jiang, X. Chen, "Plasmonic Enhanced Optoelectronic devices," Plasmonics 9, 859 (2014).

[2] E. J. C Dias, F. J. García de Abajo, "Complete coupling of focused light to surface polaritons," Optica 8, 520 (2021).

[3] P. Grahn, A. Shevchenko, M. Kaivola. "Electromagnetic multipole theory for optical nanomaterials," New Journal of Physics, **14** 093033 (2014).

[4] P. K. Jain, K. S. Lee, I. H. El-Sayed, M. A. El-Sayed. "Calculated Absorption and Scattering Properties of Gold Nanoparticles of Different Size, Shape, and Composition: Applications in Biological Imaging and Biomedicine," The Journal of Physical Chemistry110, 7238-7248(2006).

Aluminum – Zinc Oxide hybrid nanostructures for UV emission

Thomas Simon[1], **Sergei Kostcheev**[1], **Anna Rumyantseva**[1], **Jérémie Béal**[1], **Davy Gérard**[1] **and Jérôme Martin**[1]

1. Light, nanomaterials and nanotechnologies (L2n), CNRS EMR 7004, Université de Technologie de Troyes,
12 rue Marie Curie, 10004 Troyes cedex, France
E-mail: thomas.simon@utt.fr, jerome.martin@utt.fr

Aluminum nanostructures are now considered as one of the most efficient building blocks for obtaining plasmonic resonances in blue-UV. Moreover, arrays of metallic nanoparticles can sustain hybrid modes between Localized Surface Plasmon Resonances (LSPR) and grating Rayleigh anomaly, called Surface Lattice Resonances (SLR). These modes exhibit a Fano-like shape and a lower linewidth compared to the LSP mode of an isolated particle [1].

On the other hand, optical nanoantennas such as plasmonic nanostructures can significantly enhance the photoluminescence (PL) of nearby emitters. Although enhancement factors of several orders of magnitude have been reported for quantum dots or molecules, the weak spatial overlap between the emitter and the electromagnetic modes of the nanoantenna lessens the luminescence enhancement magnitude in the case of bulk materials.

Here, we study the coupling between the excitonic emission of a wide-bandgap semiconductor emitter, attached to the Al metal part, which acts as both an antenna and a light amplifier. The device we propose is composed of a solid-state ultraviolet emitter based on a thin film of zinc oxide coupled with an array of aluminum nanoparticles, as shown Fig. 1 (a). The Al nanorod array is designed to sustain SLR in the near ultraviolet. We use electron beam lithography to fabricate the aluminum nanostructures and plasma assisted sputtering to deposit ZnO thin film [2], as shown on the AFM image on Fig. 1 (b).

We experimentally demonstrate that ZnO's PL emission can be increased up to a factor of 3 with the addition of the structures, as shown Fig. 1 (c, d). We also demonstrate that SLRs are more efficient for the ZnO luminescence enhancement compared to localized surface plasmon resonances and observe the difference in behavior between possibilities in the tuning wavelength of the structure.

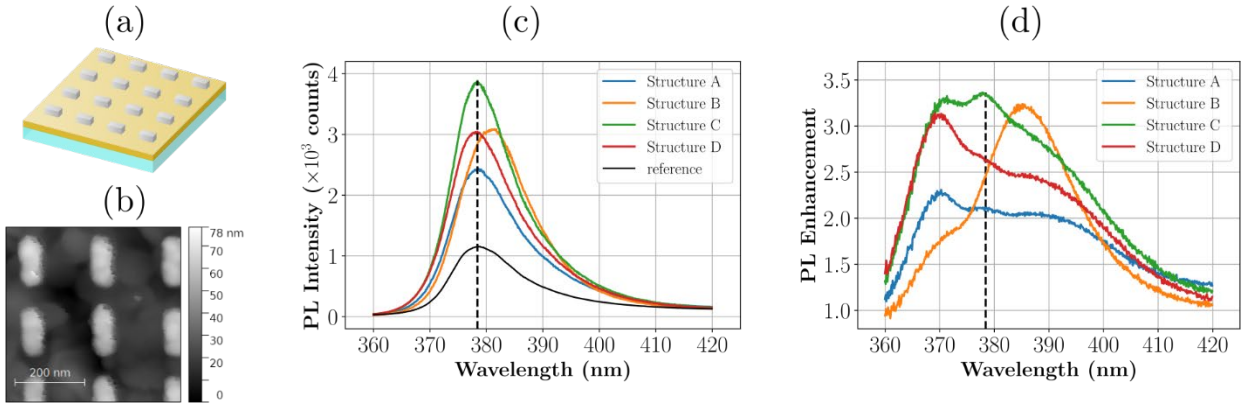

Fig. 1 (a) Schematic of the structures consisting of an array of Aluminum nanoparticles on top of a ZnO thin film. (b) AFM image of the structure. (c) Photoluminescence spectra of the ZnO film with and without the structures. (d) Corresponding enhancement spectra.

References

[1] Khlopin, D., Laux, F., Wardley, W., Martin, J., Wurtz, G., Plain, J., Bonod, N., Zayats, A., Dickson, W., and Gérard, D. 2017. *J. Opt. Soc. Am. B*, 34, 3.
[2] Simon, T., Kostcheev, S., Rumyantseva, A., Béal, J., Gérard, D, and Martin, J. 2021. *J. Appl. Phys.*, 130, 22.

Fast electrical modulation of a single plasmonic nanoresonator

Luka Zurak[1], **Jessica Meier**[1], **René Kullock**[1], **Bert Hecht**[1] **and Thorsten Feichtner**[1]

1. Nano-Optics and Biophotonics Group, Experimental Physics 5, University of Würzburg, Germany
E-mail: luka.zurak@physik.uni-wuerzburg.de

The resonance of a plasmonic nanoresonator depends on the density of free electrons n_0, as the resonant frequency of the system is proportional to the plasma frequency of the underlying material [1]. A straightforward idea to introduce a change of n_0, and thereby a change in the plasma frequency, is by means of capacitive charging. Since the capacitance for a typical nanoresonator is on the order of ten attofarads, even for applied voltages in the order of tens of volts only few hundreds of additional electrons can be pushed on the surface of the resonator. Due to the large intrinsic density of free electrons, the induced relative change in n_0 is on the order of 10^{-4}. This makes plasmonic resonances pretty robust against charging and corresponding spectral changes difficult to observe.

In order to surpass the limitations of typical capacitive systems, ion gels have been employed in earlier works leading to an increase in capacitance due to the proximity of additional ions to the metal surface [2,3]. However, one of the drawbacks of this approach is a very slow switching time as well as occurrence of hysteresis which likely originate in surface chemistry effects [3].

Here, we demonstrate fast electrical modulation of the plasmonic resonance of a single electrically connected gold nanorod. We employ lock-in techniques to measure the relative change of the scattering signal $\Delta S/S_0$ in the spectral range from 500 to 900 nm, while driving our structure with up to 50 kHz in frequency and up to 30 V in voltage amplitude. The obtained results are of the expected order of magnitude according to existing theories, which we discuss in detail. Our results form the basis for the thorough understanding of numerous effects in earlier publications including the so-called plasmoelectric potential [4].

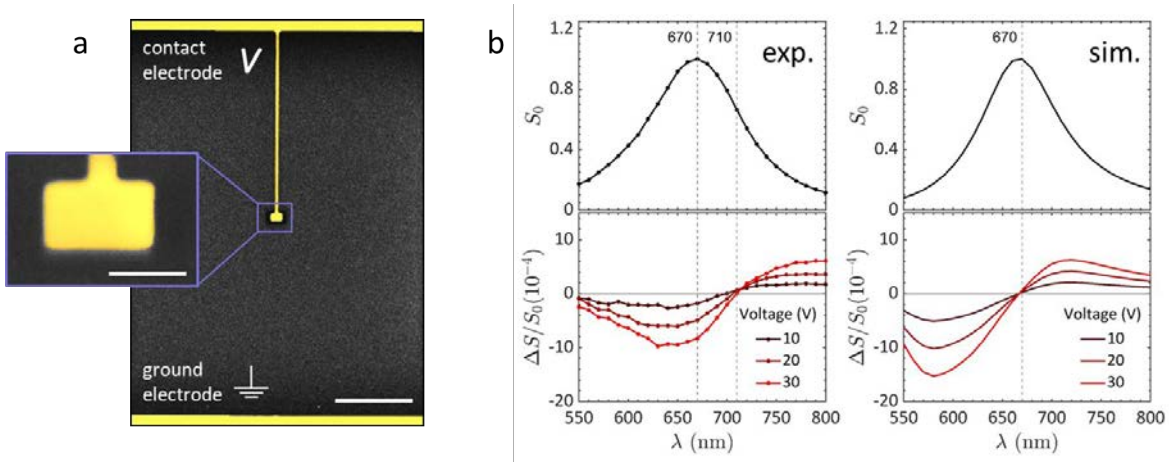

Fig. 1 a) Colored SEM images of the electrically connected gold nanoresonator for capacitive charging. Scale bar is 500 nm, and 100 nm in the inset. b) Unchanged scattering spectra S_0 (top) and relative change of scattering $\Delta S/S_0$ under applied potentials (bottom), in experiment (left) and simulation (right).

References

[1] Biagioni, P., Huang, J. S, Hecht, B. 2012 *Rep. Prog. Phys.,* 75, 1-40
[2] Collins, S. S. E., Wei, X., McKenzie, T. G., Funston A. M., Mulvaney, P. 2016 *Nano Lett*., 16, 6863−6869
[3] Maniyara, R. A., Rodrigo, D., Yu, R., Canet-Ferrer, J., Gosh, D. S., Yongsunthon, R., Baker, D. E., Rezikyan, A., Garcia de Abajo, F. J., Pruneri, V. 2019 *Nat. Photon*., 13, 328-333
[4] Sheldon, M. T., Van de Groep, J., Brown, A. M., Polman, A., Atwater, H. A. 2014 *Science*, 346, 828-831

Fractal-like multiresonant aluminum optical antennas – the Cayley Tree

Thomas Simon[1], **Xiaoyan Li**[2], **Jérôme Martin**[1], **Dmitry Khlopin**[1], **Odile Stéphan**[2], **Mathieu Kociak**[2] **and Davy Gérard**[1]

1. Light, nanomaterials and nanotechnologies (L2n), CNRS EMR 7004, Université de Technologie de Troyes, 12 rue Marie Curie, 10004 Troyes cedex, France
2. Laboratoire de Physique des Solides, Bâtiment 510, UMR CNRS 8502, Université Paris Saclay, Orsay 91400, France
E-mail: thomas.simon@utt.fr, jerome.martin@utt.fr

An optical antenna is a nanostructure that can convert an incident free radiation into a localized excitation, and the reciprocal. Being able to perform different functions, such as entrance and exit ports, energy harvesting systems, directional emitters, or substrates for enhanced spectroscopies, they have become vastly used as building blocks for nanophotonic devices [1]. Optical antennas are usually made with resonant nanoparticles, whether metallic or dielectric, but it is still a challenge to obtain structure exhibiting multiple broadband resonances, over a large span of wavelengths. This kind of structures could be interesting for fields such as nonlinear optics or multiple harmonics generation.

Here, we studied a self-similar, fractal-like structures, known as the Cayley Tree, as broadband optical antennas [2]. The aluminum nanoparticles based on this specific shape were fabricated using electron beam lithography on TEM compatible substrate (15-nm-thick Si_3N_4 membranes). Using Electron Energy Loss Spectroscopy (EELS), we experimentally evidenced that a single aluminum Cayley tree, a simple self-similar structure, sustains multiple plasmonic resonances. The comparison with Finite Difference Time Domain (FDTD) simulations allowed us to distinguish between bright "extremity" modes and dark "core" modes [3].

We experimentally observed that the spectral position of these resonances spans over a wide range of frequencies, from ultraviolet to thermal infrared, and can be tuned by adapting the length of the different parts of the particle. As such, Cayley Tree based nanostructures would be of high interest in a variety of applications as photodetection, light harvesting, surface-enhanced spectroscopy and even nonlinear optics.

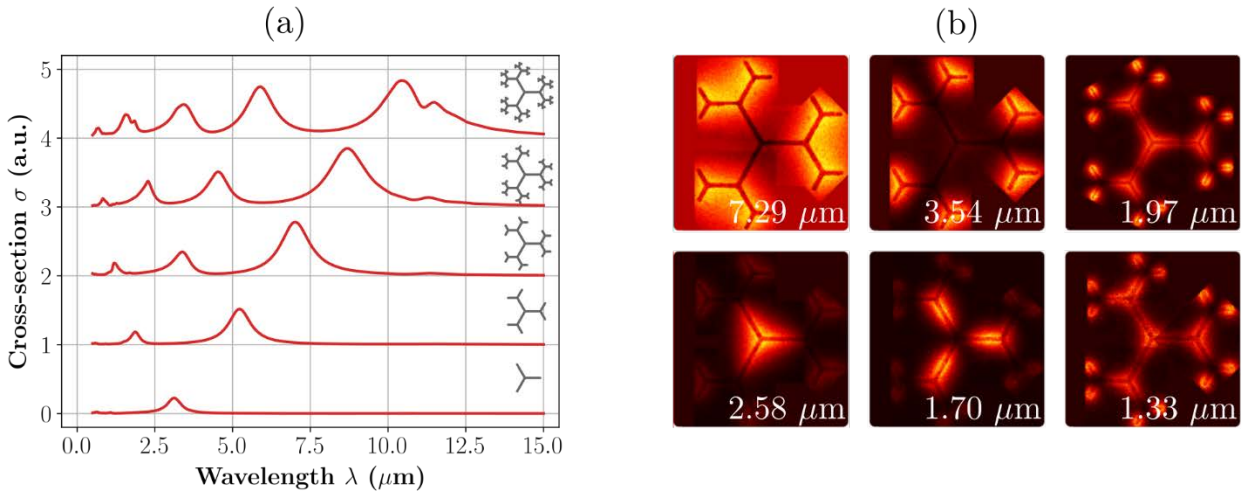

Fig. 1 (a) Schematic FDTD-simulated extinction spectra for aluminum Cayley trees with different generations. (b) Energy-filtered EELS maps at different resonance wavelengths for a Cayley Tree of generation 3, showing the bright "extremity" modes (upper three) and dark "core" modes (lower three).

References

[1] Novotny, L., & Van Hulst, N. 2011. *Nat. photonics*, 5, 2.
[2] S. Gottheim, H. Zhang, A. O. Govorov, N. J. Halas. 2015. *ACS Nano*, 9, 3.
[3] Simon, T., Li, X., Martin, J., Khlopin, D., Stéphan, O., Kociak, M., Gérard, D. 2022. *Proc. Natl. Acad. Sci. U.S.A.*, 119, 4.